Energy saving screen materials

Measurement method of radiation exchange, air permeability and humidity transport and a calculation method for energy saving

Silke Hemming, Esteban Baeza, Vida Mohammadkhani and Bram van Breugel

Report GTB-1431

WAGENINGEN
UNIVERSITY & RESEARCH

LTO Glaskracht Nederland

Ministerie van Economische Zaken

KAS ALS ENERGIEBRON

Referaat
De doelstellingen van het project waren het kwantificeren van in kassen gebruikte scherm eigenschappen (emissie en transmissie voor warmtestraling, luchtdoorlaatbaarheid en vochttransport) en de bepaling van de totale energiebesparing onder gedefinieerde omstandigheden om de prestaties van verschillende schermen (en leveranciers) met elkaar te kunnen vergelijken. Dit helpt telers om meer informatie te krijgen over relevante scherm eigenschappen en stelt hen in staat om een weloverwogen keuze voor een investering te doen. De resultaten tonen aan dat ondoorlatende schermen en schermen met lage emissie en transmissie voor warmtestraling de hoogste energiebesparing geven. Doorlaatbare schermen geven de hoogste vochtafvoer en de laagste luchtvochtigheid tijdens scherm gebruik zonder de noodzaak voor extra mechanische ontvochtiging.

Abstract
The objectives of the project were the quantification of the greenhouse screen properties (emissivity and transmissivity for thermal infrared radiation, air permeability and humidity transport) and the determination of the total energy saving under defined conditions in order to be able to compare the performance of different screens (and suppliers) with each other. This helps growers to understand more about screen properties and allows them to make an informed choice of investment. The results show that impermeable screens and screens with low emissivity and low transmissivity for thermal infrared radiation give highest energy saving. Permeable screens give highest transport for humidity and lowest air humidity during screen usage without the need for additional mechanical dehumidification.

Reportinfo
Report GTB-1431
Projectnumber: 3742 2263 00
DOI number: 10.18174/409298

Disclaimer

Address

Wageningen University & Research, BU Greenhouse Horticulture
Violierenweg 1, 2665 MV Bleiswijk
P.O. Box 20, 2665 ZG Bleiswijk
The Netherlands
+31 (0) 317 - 48 56 06
+31 (0) 10 - 522 51 93
glastuinbouw@wur.nl
www.glastuinbouwur.nl/glastuinbouw

Table of contents

Summary

Screens are used in practice in various types (woven fabrics, knitted fabrics or foils, open or closed structures, transparent, diffuse, aluminized or various colours) and for various purposes (energy saving, reduction in light sum or light diffusion). An important goal of screens in Dutch greenhouses is energy saving. Unfortunately, there is until now no **objective method to determine the energy saving** of a screen under defined conditions.
In this study, different methods and procedures for determining single screen material properties have been evaluated and developed. The total energy saving of a screen materials is determined by the radiation exchange (transmissivity and emissivity of heat radiation), the air permeability through the screen (convection at low wind speeds) and the humidity transport through the material (air and with that humidity transport and humidity transport in threads or plastics by diffusion, absorption or adsorption). It is necessary to measure all of these screen properties under controlled conditions and then use a physical model to calculate the energy performance for screens for a defined situation. In this way, materials can be compared with each other.
The goal of the project is the development of appropriate measuring methods, protocols and a calculation method for material comparison. Further, the objectives of the project were the quantification of the greenhouse screen properties (emissivity, air permeability and humidity transport) and the determination of the total energy saving under defined conditions for different selected screen materials.
The **emissivity** of selected screen samples has been measured on the earlier developed TNO Emissivity measurement device (De la Faille *et al.,* 2009). Emissivity values largely differ between screen materials. While investigated materials BP16A and NT16D had very low emissivity values (<10%), others like NT16K, LS16U and CU16O showed medium or high values (NT16H and NT16M, >60%). Emissivity values can be different on both sides of a screen material depending on the material composition. Next to that, screens NT16M, NT16H and also NT16D and CU16O show a low transmissivity for infrared radiation. However, only NT16D shows a combination of low emissivity and low IR transmissivity, resulting in a high IR reflectivity. A combination of low emissivity and low transmissivity for infrared radiation (high reflectivity) in general result in a high energy saving.

Air permeability of screens has been measured both at low wind speeds on the WUR Air suction device and at high wind speeds in a wind tunnel at the University of Almeria. Air permeability is largely depending on the screen materials composition. While materials CU16O (glassfibre non-woven), NT16E (porous with 4 aluminum strips) and NT16F (porous with 2 aluminum strips) have an extremely high air permeability, while LS16U (knitted with transparent strips), NT16M (glassfibre woven), NT16H show a medium permeability, others like NT176D (laminated with transparent and aluminium strips) and BP16A (transparent woven) have an extremely low air permeability. In general, a low air permeability leads to higher energy saving both through lower sensible heat loss and latent heat loss.

In commercial greenhouse measurements of the air velocity have been carried out with 3D anemometers for different scenarios of ventilation and screens opening percentages. We can conclude that if energy screens are used and with greenhouse natural ventilation openings usually open at low percentages, the measured values of the vertical resultant of air velocity vector near the screens are below 0.1 m s^{-1} for the majority of time, although at some specific periods they also can reach values between 0.1-0.2 m s^{-1}. Therefore, and for the purpose of characterizing the air permeability values of the different screens, a range of air velocities lower than 0.2 m s^{-1} should be suffice to characterize the screens aerodynamic properties properly. Air suction device measurements at low wind speeds are appropriate. Wind tunnel measurements at high air speeds are not needed to characterise screen performance in greenhouse practice.

Humidity transport has been measured by two different measurement principles. In cup method, a gradient of absolute humidity is maintained on two sides of the screen sample, water has to diffuse through the specimen following the water vapour gradient. With the cup method, the water vapour transmission rate (WVTR) is measured according to ASTM E96.

One of the limitations of the cup method is that it only accounts for one of the transport mechanisms through a porous material (here a greenhouse screen), that is diffusion. However, in practice, greenhouse energy saving screens are located in greenhouses generating two different volumes, one below the screen, where the heating system and crop transpiration generate a warmer and more humid environment and one above the screen which is colder and dryer. This means that there is a temperature gradient next to a water vapour gradient. This means that there will be airflow through the screen driven by natural or forced convection (depending on the opening of natural ventilation vents and on the presence of fans) depending on the air permeability of the screen. This convective airflow will also transport water vapour with it, which is not quantified by the cup method. In addition, the temperature gradient on both sides of the screen will also lead to condensation on the inner part of the screen when screen temperature will be lower than dew point temperature. When condensation occurs, part of the water is transported through the screen and re-evaporated on the other side, accounting for an extra mechanism which is also not quantified by the cup method. As a consequence, a new measuring equipment and protocol should be used that accounts in a more realistic way for the conditions normally encountered in a greenhouse and which is able to quantify total humidity transport through greenhouse energy saving screens. Swerea Institute, Sweden, has developed and specific method (Swerea IVF 82-11) to perform these types of measurements in a climate box.

Results indicate that the humidity transfer values measured under the conditions of the Swerea method are higher than those measured using the cup method. This proves that humidity transport is a combination of diffusion and other two mechanisms, convection and condensation/transport/re-evaporation. Screens NT16D and BP16A show a low humidity transport, others show intermediate values such as SL16U, NT16H and NT16M, CU16O shows the highest humidity transport measured. In general, a low humidity transport relates to a higher energy saving. However, it might be necessary to use an additional dehumidification device to meet crop requirements.

The **total energy saving of screens** is strongly related to the materials properties, such as emissivity, air permeability and humidity transfer. The model KASPRO (de Zwart, 1996) is used for overall energy saving calculations under pre-defined conditions.
In general, the use of any energy screen saves energy compared to a greenhouse without a screen.
The results of calculated energy saving of the selected screens show a clear relation between the air permeability values of each screen and their energy saving. Through buoyancy, diffusion and convection processes warm and humid air is transported through a permeable screen, with that sensible and latent heat is removed from the greenhouse. The result is an energy loss which is depending on the amount of air permeability.
The result of calculated energy saving of the selected screens shows also a clear relation between the emissivity values of each screen and their energy saving. Hot heating pipes, warm crops and installations exchange heat radiation with the cold greenhouse roof and the cold sky. When the screens are closed, part of the thermal infrared (heat) radiation from inside the warm greenhouse is absorbed and emitted by the screen material. That means that the radiative heat losses are reduced towards the cold roof and outside the greenhouse. The reduced energy loss is depending on screen emissivity.
Screen NT16D shows highest total energy savings with an average saving of ca. 25% (based on energy consumption of all hours, only 2664 h were screen hours) or ca. 48% based only on the night hours in which screen is used. This screen has a low air permeability, a low emissivity and low transmissivity for infrared radiation combined. Screen BP16A, LS16U, NT16H, NT16K and NT16M showed yearly average saving so ca. 14-17% or ca. 25-30% based only on the night hours in which screens are used. Lowest energy saving was calculated for CU16O, this screen has the highest humidity transport. Screens NT16D and BP16A show the highest maximum energy saving during the coldest night. Both screens show the lowest humidity transport leading to high energy saving. However, during peak hours of crop transpiration humidity transport through the screens is smaller than transpiration, showing the importance of using some kind of mechanical dehumidification system if very impermeable screens are used. In general, energy consumption by mechanical dehumidification systems is much lower than additional energy saving of impermeable screens leading still to the highest energy saving of screens with low air and humidity permeability.

From the project results we recommend **screen producers** to obtain the following material properties for their materials and provide this information to growers. Growers can use this information to make a choice for a screen material depending on crop and requirements.

- Emissivity of screens.
- Air permeability of screens.
- Humidity transport of screens.
- Calculation of total energy saving key figures.

Emissivity ε should be reported next to IR transmissivity τ_{IR} and IR reflectivity r_{IR}, all in %. TNO emissivity meter can be used as equipment. A procedure is given in this report.
Air permeability should be reported in terms of permeability K, in m^2. A figure of permeability depending on air velocity should be given. An air suction device can be used to determine air permeability of screens for low air velocities. A description of the equipment is given in this report. A measurement procedure is given in this report.
Humidity transport of screens should be measured following the Swerea method. The cup method is not suitable. A description of the experimental set-up and measurement procedure is given in this report. Results should be reported in water vapour transport in $g/m^2/h$.
Total energy saving of screens should be calculated with KASPRO. The assumptions given in this report should be used for calculations. The same key figures for total yearly energy consumption, total yearly energy saving, energy saving during night hours and maximum saving should be reported. Next to that a figure of expected daily humidity transport through the screen should be reported.

Growers can select a specific screen material based on single screen material properties and total energy saving potential. Impermeable screens and screens with low emissivity and low transmissivity for thermal infrared radiation give highest energy saving. However, additional mechanical dehumidification might be needed depending on the crop requirements. Permeable screens give highest transport for humidity and lowest air humidity during screen usage without the need for additional mechanical dehumidification.

1 Introduction

Screens are used in practice in various types (woven fabrics, knitted fabrics or foils, open or closed structures, transparent, diffuse, aluminized or various colors) and for various purposes (energy saving, reduction in light sum or light diffusion). An important goal of screens in Dutch greenhouses is energy saving. Unfortunately, there is until now no objective method to determine the energy saving of a screen under defined conditions. Energy savings rates are estimated by producers using different methods. Growers have few opportunities to get objective information on screen performance and to compare screens with each other in order to derive at a balanced investment decision.

The problem of lack of comparable information is not new. Earlier the project "Emission Values screens", has been carried out by TNO, WUR and two screen manufacturers. This has led to an objective measurement method and device for the determination of the emissivity of screens. However, this is not sufficient to determine the total energy saving of screens. The total energy saving is determined by the radiation exchange (transmissivity and emissivity of heat radiation), the air permeability through the screen (convection at low wind speeds) and the humidity transport through the material (air and with that humidity transport and humidity transport in threads or plastics by diffusion, absorption or adsorption). It is necessary to measure all of these screen properties under controlled conditions and then use a physical model to calculate the energy performance for screens for a defined situation. In this way, materials can be compared with each other. The goal of the project is the development of appropriate measuring methods, protocols and a calculation method for material comparison.

The final energy saving in practice, however, also depends on the screen installation and the usage by the grower (screen timing, number of screen hours), which will not be covered here. Also, ageing and condensation will further influence screen performance in practice. In the future, it makes sense to carry out comparative measurements of different materials with known properties in a practice.

The objectives of the project were the quantification of the screen properties (emissivity, IR transmissivity, air permeability and humidity transport), and the determination of the total energy saving under defined conditions in order to be able to compare the performance of different screens (from different suppliers) with each other. This helps growers to understand more about screen properties and allows them to make an informed choice of investment. This will promote the use of insulating screens in practice, helping to implement HNT. Due to a more conscious handling of screens growers can realise energy savings up to 5%. Quantification of different screen properties and overall energy saving of different screens (and suppliers) in an objective way, provides manufacturers with more information and helps them to develop even better products in the future.

2 Materials and methods

2.1 Energy saving screen materials

In order to have a realistic view on measurement methods and their limitations, it is decided to select a wide range of energy screens with different properties made by different producers. The available screens can be divided in different groups on base of used material, fabricating method, application or a combination of those:

- Transparent screens.
- Aluminized screens.
- Various grades of porosity.
- Various grades of diffusion.
- Black-out screens.
- Assimilation screens.
- Different ways of manufacturing: knitted or woven.

We have received 29 screens with different properties from all producers. A complete list of samples with WUR codes and descriptions provided by producers can be found in Annex 1 Overview of samples. Because of the similarities between some samples and the goal to develop a general procedure, we have selected 7 screens with different and challenging characteristics to measure. This selection is based on differences in porosity, structure (weaving techniques or composition of different materials in one screen) and basic material. In Figure 1 an overview of the 7 selected screens is presented.

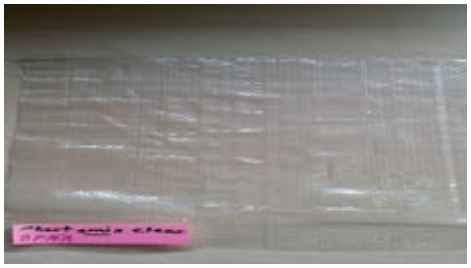

Phormitex Clear /BP16A.

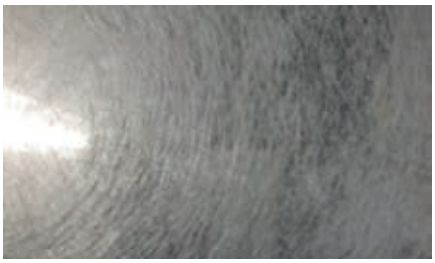

AT40 , thin version of glassfibre sample /CU16O.

Luxous 1347 FR /LS16U.

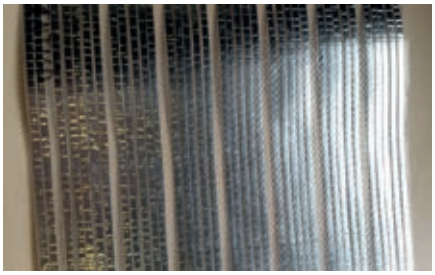

SHS Woven Clear mit Alustreifen /NT16D.

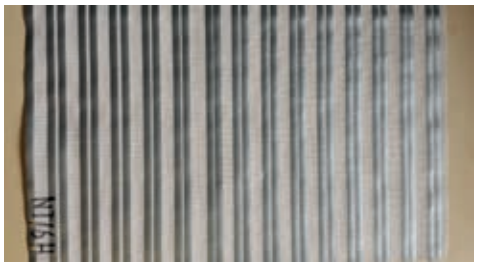

HS 885 ANTIFIRE B1 Trevira met 2 Streifen /NT16H.

SHS 15 ANTIFIRE B1 /NT16K.

Glasfasergewebe /NT16M.

Figure 1 *Overview of 7 selected screens.*

2.2 Measurement of radiometric properties

2.2.1 Background

Thermal infrared radiation (IR) is heat radiation in the range of 2500-100000 nm or 2.5-100 mm. When thermal infrared radiation hits a material, part of it is transmitted (τ_{IR}), a part is reflected (r_{IR}) and a part is absorbed ($a_{IR}=\varepsilon$) by the material. This energy exchange process can be formulated as follows:

$$\tau_{IR} + a_{IR} + r_{IR} = 1$$

This means that when thermal infrared radiations coming from the greenhouse hits a screen material, its IR transmissivity (τ_{IR}), IR reflectivity (r_{IR}) and the emissivity (ε) determine the height of the barrier the screen forms for radiative heat loss.

2.2.2 Emissivity measurement device

The emissivity measurement device has been developed in the past by TNO in order to measure the thermal radiative properties (2.2.1) of greenhouse screens. The device consists of two radiative half spheres kept on different temperatures. One half sphere has the room temperature and the other one is heated up. The temperature difference is about 25 to 30 degrees Celcius. Both half spheres have a built-in infrared sensor. The sensor consists of a large number of thermo-couples which are integrated on an IC. Herewith any increase or decrease in surface temperature is compared with the sensor temperature. The sensor is able to measure its own temperature and has a response time less than 0.1s. Emissivity (ε), thermal infrared reflectivity (r_{IR}) and thermal infrared transmissivity (τ_{IR}) are determined based on the known properties of glass and gold which are measured during calibration, as well as the reading of the empty device.

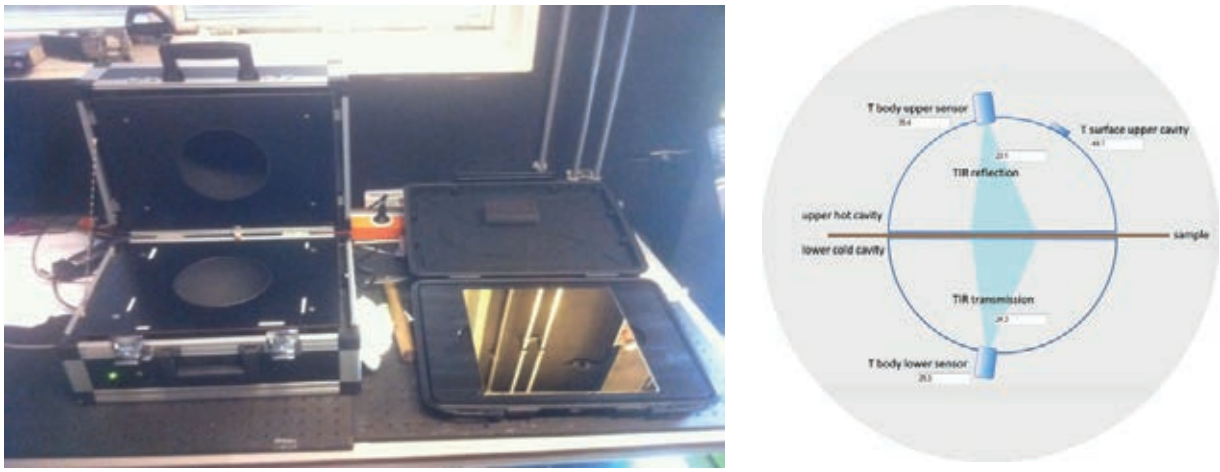

Figure 2 *Picture and schematic drawing of the emissivity measurement device (TNO).*

The following specifications are given on the device:

- The device measures in between hemispherical and near normal values. By default, hemispherical values are used. The error depends on the material properties of the measured sample and is largest for smooth flat materials, around 2% for samples with IR reflectivity around 50%. For screens the error is estimated to be smaller.
- For highly transparent samples (>50% IR Transmissivity) the IR reflectivity of the spheres should be taken into account. The IR reflectivity of the spheres is estimated to be around 10%. A different algorithm is needed to measure highly transparent samples. In that case TNO has to be contacted.
- The Melexis sensors have a sensitivity for different thermal infrared wavelengths as in the following figure. The sensitivity of the sensors covers the range of 4-14μm. Results can therefore differ from other devices such as an FTIR spectrophotometer.

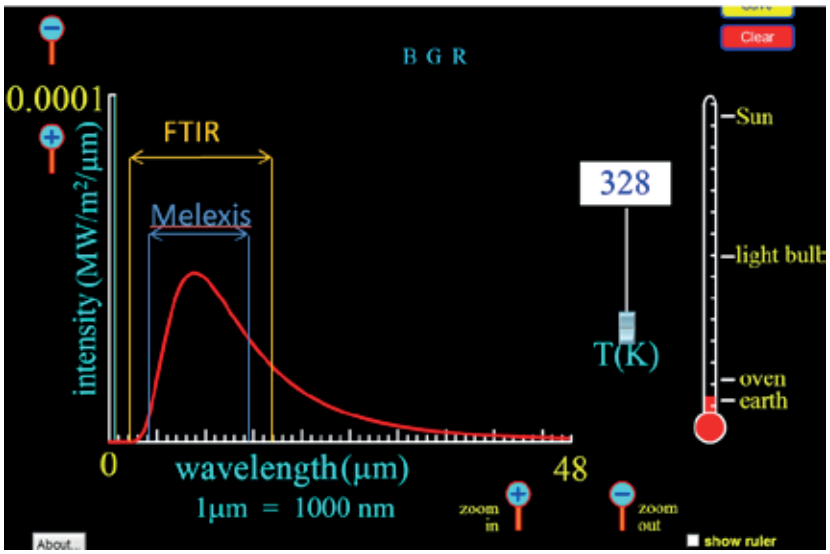

Figure 3 *The Melexis sensors window.*

2.2.3 Measurement procedure

The measurement must be carried out in a room with a stable and controlled climate. High air velocities, such as air streams from open windows or doors or even passing people, will disturb the temperature balance between the cavities and influence the measurements.

0. Sample preparation.
   - Cut a piece of unfolded screen sample in A4 format.
   - Keep the sample on room temperature during the measurements.

1. Connection and power.
   - Connect the device with the USB cable to the dedicated computer.
   - The green led is on and the red led starts blinking.
   - Check the communication with the computer (see also 1 – Status connect).
   - Plug in the 230V power plug to start the heating / fan system of the device.
   - Keep the device in an open position during the heating up process to protect the lower sphere from warming up.
   - When the device is warming up the red led keeps blinking.
   - When the device is heated up the red led stays on continuously.
   - The system further controls the cavity temperature, do not unplug the 230V.

Figure 4 *Green and red LED on device.*

2. Status connect
   - Start the program by clicking the “TNODevice_V0.7.exe” file.
   - Click button “Connect monitor”.
   - Check if the COM Port is found in field “Port”.
   - Check if raw data is being received (in field “Connection”).
   - Check if measured temperature values in figure are present (and changing).
   - The status line also displays the instructions during this process.

3. Reference material

   3A
   - Measure the IR temperature with the reference sample, gold side facing upwards.
   - The hot sphere should be on temperature before this step.
   - Place the sample and click “A”.
   - The status line also displays the instructions during this process.
   - Close the device to start the measurement.
   - Open the device directly after the measurement, a graph pops up automatically.
   - Check for any irregularities; if the graph shows irregularities, remove the sample and wait a few minutes until the cavity temperatures are stable again and repeat the measurement.

   3B
   - Measure the IR temperatures with the reference sample, glass side facing upwards.
   - Place the sample and click “B”.
   - Close the device to start the measurement.
   - Open the device directly after the measurement, a graph pops up automatically.
   - Check the graph for irregularities, if necessary repeat the measurement.

   3C
   - Measure without a sample for IR transmissivity reference.
   - Remove the reference sample.
   - Click button “C”.
   - Close the device to start the measurement.
   - Open the device directly after the measurement, a graph pops up automatically.
   - Check the graph for irregularities, if necessary repeat the measurement.
   - Part of the results of the measurements in step 2 are also used in the formulas for the calculations of the IR reflectivity, emissivity and IR transmissivity of samples during measurements in step 3.
   - Information of the physical background, working principle of the device and calculation formulas can be found in a (Dutch) TNO report: http://tuinbouw.nl/project/u-waarde-schermdoek.

4. Sample measurement
   - Place a sample to be measured.
   - Click button "Measure".
   - Close the device to start the measurement.
   - Open the device directly after the measurement, the graph pops up automatically.
   - The status line also displays instructions during this process.
   - Between measurements, measure a clear EFTE sample, if the emissivity value varies more than expected. (±2%) repeat calibration for higher accuracy.
   - Protect the cold sphere from heating up.
   - Check the graph for irregularities.
   - The 0 on the time axis corresponds with the used values for the calculation of IR reflectivity, emissivity and IR transmissivity of the sample.
   - The values are calculated and displayed in the corresponding yellow fields.
   - The graph can be saved to the clipboard using the top-left button of the graphical program and copied to various programs.
   - The text file "OutputKoffer.txt" in the used folder on the computer contains the corresponding data of the graph in tabular format.
   - In the text file the moment of closing of the device can be checked (at point 0 the status changes from 0-open to 1-closed), if necessary repeat the measurement.
   - Pay attention: both graph and table will be overwritten during following measurements.

- The last graph can always be recreated by clicking the "Graph" button (for instance in case the graph is closed unintendedly).
- The given date and time are of the moment of the (re)creation of the graph (not of the moment of the measurement itself).
- During measurements, the reference procedure (step 2A, 2B, 2C) should be repeated regularly in order to be ensure correct reference values since measurement conditions might have been changed during time (e.g. after a break or when the ambient room temperature has increased.

5. Measurement result
   - Emissivity ε, IR transmissivity τ_{IR} and IR reflectivity r_{IR} of a screen material surface.

2.3 Measurement of air permeability

2.3.1 Background

In a greenhouse with screens air exchange takes place between both sides of the screen materials (crop area and roof area) if the screen installation is closed. These air exchange properties of the screen material are important to characterise because air flow causes sensible and latent heat flow through the material and therefore energy and water vapour losses to the top greenhouse compartment. In order to accurately determine how much air is exchanged through a material the air permeability of a material has to be measured under defined conditions in the laboratory.
The permeability of a screen material can be characterised by generating a set number of air velocities through the screen (e.g. wind tunnel 2.3.3 or air suction device 2.3.4) and recording the resulting pressure difference over the screen. The measurement data obtained is then used to calculate the permeability and inertial factor, two characteristics that determine air transport.
The relation between the air velocity (υ) and the pressure difference over a screen follows a combination of a linear and a quadratic relationship, the Forchheimer-Darcy equation, in which the linear Darcy term is dominant at low speed laminar flow and the quadratic term is the dominant effect at more turbulent higher air speeds.

$$\frac{\partial P}{\partial x} = \frac{\mu}{K} u + \rho \left(\frac{Y}{K^{1/2}} \right) |u| \, u$$

where P is the air pressure (Pa), χ is the thickness of the screen materials (m), μ is the dynamic viscosity (Pa s), K is the permeability of the screen (m^2) and Y is the Inertial factor (-), ν is the air velocity (m/s) and ρ is the air density (kg/m^3).
To solve the properties the measurement data is fitted into a quadratic polynomial

$$C1 \cdot \nu + C2 \cdot \nu^2 = P$$

The solved coefficients are then used to calculate respectively the permeability (K) and Inertial factor (Y) via

$$K = \frac{\mu}{C1}$$

And

$$Y = \sqrt{\frac{\mu}{C1}} \cdot \frac{C2}{\rho}$$

2.3.2 Measurement of air velocities in greenhouses

First the air velocities to be expected to occur in a greenhouse have to be determined. The knowledge of the vertical component of air velocity near the screens under a range of scenarios is important in order to select the appropriate velocity range under which the air permeability of the screens has to be measured in the laboratory. Screens can be used under natural ventilation conditions (greenhouse vents partially open or fully closed) or under forced ventilation conditions (fans in greenhouses). In order to determine air velocities under natural ventilation conditions, anemometry techniques can be used to measure conditions in greenhouses. Air velocities under forced ventilation conditions can be calculated. No research work can be found in literature in which anemometry techniques have been used in order to study the airflow near the energy saving screens in greenhouses. Therefore, an experiment was carried out to characterize the air velocities near different types of screens in commercial greenhouses using ultrasonic 3D anemometers.

The first set of measurements was performed in a commercial greenhouse in Maasdijk (The Netherlands) (Figure 5). This company (Hofland freesia) has two large glasshouse compartments in which they grow *Freesia sp.* Measurements were carried out in the compartment marked in red in Figure 5. This greenhouse compartment is a standard Venlo glasshouse with 8 m bays. The greenhouse has Venlo roof vents of 3.2 x 1.2 m and two types of screens:

- A shading screen (Harmony 5220 O FR, Svensson)
- An energy saving/black-out screen (Obscura 9950 FR W, Svensson)

Before installing the 3 ultrasonic 3D anemometers (model Windmaster 3 axis ultrasonic anemometer, Gill instruments, Range 0-50 m/s, Resolution 0.01 m/s, Accuracy* <1.5% RMS @12 m/s), they were calibrated in a simple wind tunnel in Wagenigen University & Research Greenhouse Horticulture lab (Figure 7).

Figure 5 *Air view of the greenhouse compartment from Hofland freesia (marked in red) where measurements were performed.*

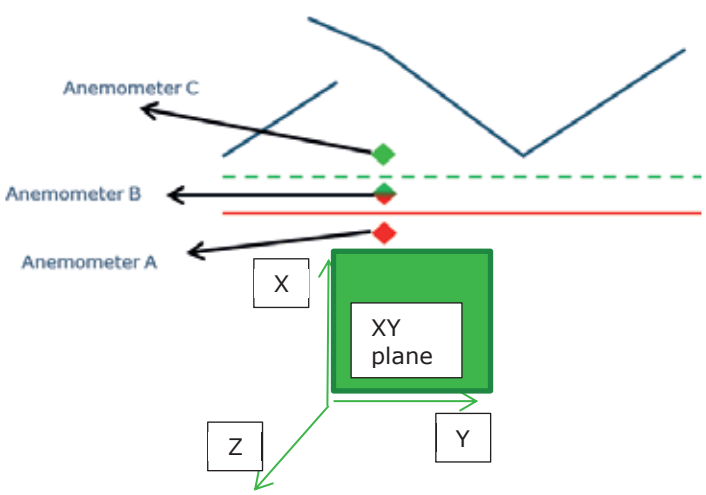

a. Scheme of the disposition and location of the sonic anemometers in the commercial greenhouse.

b. Placement of the sensors in the greenhouse.

Figure 6 *Location of the three sonic 3D anemometers in the commercial greenhouse.*

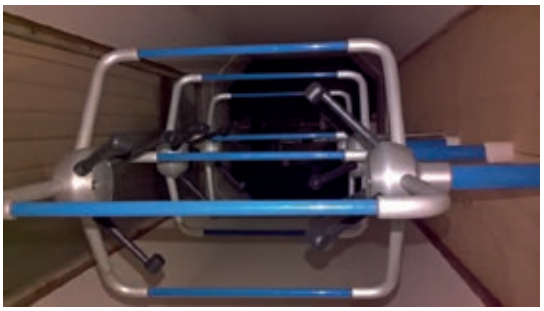

a. Wind tunnel and three anemometers.

b. Three anemometers inside wind tunnel test section.

Figure 7 *Details of the calibration process of the three ultrasonic 3D anemometers in the lab.*

For the measurements in the greenhouse, only the vertical component of air velocity vector (that in the XY plane) is of interest as it is the one contributing to the mass and energy exchange through the screens. Therefore, only the components of the air velocity vector in the XY plane were calibrated (from now on, U and V components) with measurements from a very precise hot wire anemometer (Velocicalc plus multi-parameter ventilation meter 8386, TSI), results showing a very good agreement between the three sensors (named a, b and c) (Figure 8), with some minor deviations for the b sensor values higher than 2 m s^{-1}, higher than those expected to be measured inside the greenhouse, which should be in a much lower range (Wang *et al.,* 1999; Molina-Aiz *et al.,* 2009).

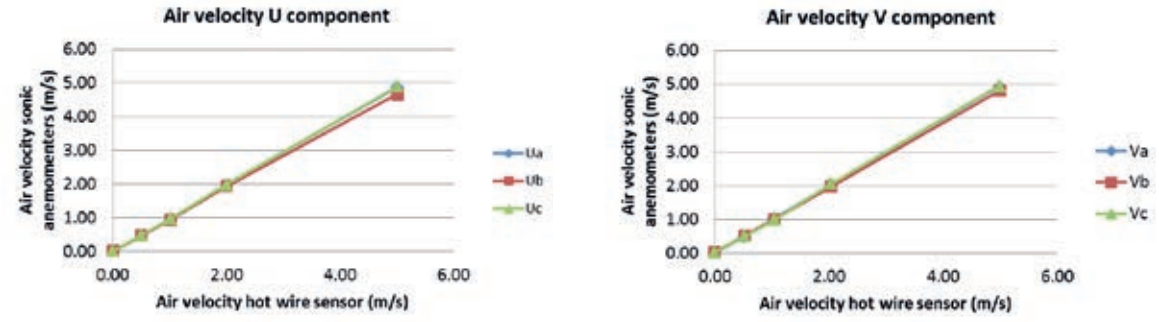

a. U component air velocity module (hot wire vs sonic anemometers).

b. V component air velocity module (hot wire vs sonic anemometers).

Figure 8 *Calibration of air velocity sonic anemometer.*

Once calibrated, sensors were finally installed in the commercial greenhouse following the arrangement that can be seen on Figure 7. The 3 sensors were completely aligned vertically; sensor *c* was located immediately above the top screen (the shading screen); sensor *b* was located in between both screens; and sensor *a* was located below the lower screen (the energy saving/black-out screen). Sensors were located also exactly below the centre of one roof vent, so it can be expected that, when vents were open the air exchange through natural ventilation can be seen in larger air velocity values, with some dependency on external wind speed.

Sensors remained in the greenhouse between September 9 and October 25, 2016. The vertical component of air velocity (in the XY plane) was calculated for each sensor (a, b and c) as

$$R_{\{a,b,c\}} = \sqrt{U^2 + V^2}$$

In order to account for the effect of the external wind velocity, for the moments when vents were open, the values of normalized air velocity V_{norm} were obtained dividing the resultant in the XY plane by the external wind velocity v_{wind}:

$$V_{norm} = \frac{R_{\{a,b,c\}}}{v_{wind}}$$

2.3.3 Windtunnel, high air velocities

In order to characterize the pressure loss through all 29 screen samples obtained from the companies, at a range of high air velocities, samples were sent to the LABORATORY FOR QUALITY CONTROL AND EVALUATION OF AGROTEXTILES of the University of Almería, Spain. This laboratory has a small wind tunnel that allows measuring the pressure loss caused by materials as a function of the air velocity in a range of 0-10 m s^{-1} (Figure 9).

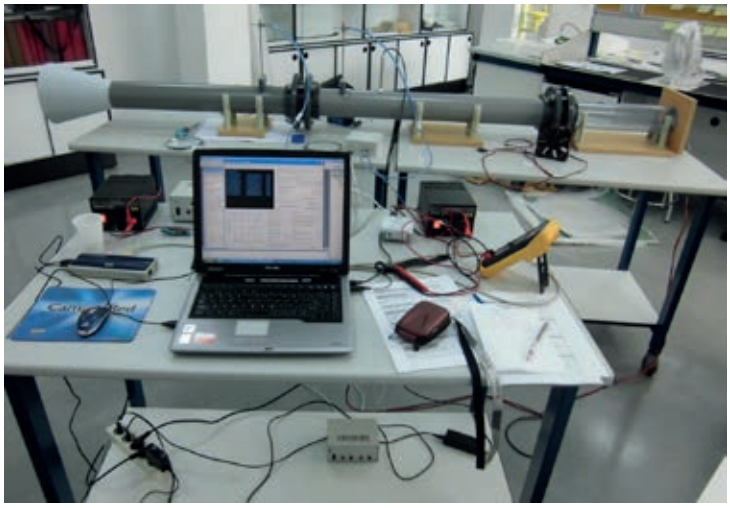

Figure 9 *Experimental set up of the wind tunnel.*

For the static pressure measurements, two Pitot tubes of 4 mm diameter (Airflow Developments Limited) are placed upstream and downstream of the screen sample. The static pressure outlets of both Pitot tubes are connected to two different differential pressure transducers, since for some screens the range of 0-200 Pa of the first transducers is too small to characterize high enough air velocities (Special Instruments, 0-200 Pa; Delta Ohm 0-1000 Pa). The air velocity is measured using a thermal anemometer with an adjustable scale (1, 2, 10, 20 m/s) (Delta Ohm, 0-10 m/s). Air is moved by a DC fan (NBA-MAT, Minesbea co., Ltd., mod. 4715KL-04W-B40). The air speed is generated by means of PWM (pulse with modulation) technique. Summarizing, a square wave is generated and its frequency can be changed as well as the active/inactive ratio. The management of the wind tunnel is carried out by a software called Boreas v1.3, that allows for full automation of the test, that is, no need to be present during the measurements.

To perform the measurements the air velocity boundaries (i.e. 0-4 m/s) are established, as well as the number of intervals (i.e. every 0.2 m/s) and the number of readings for each series (i.e. 30). In order to improve the results the device measures increasing air speed from 0-4 m/s but also decreasing from 4-0 m/s. At the end of each measuring series, the air speed is modified, and after a lapse, the software checks that the flow is stable (i.e. that between two consecutive measurements (10 s) the difference in air speed is lower than 0.05 m/s; if not, it waits and checks again); when the flow is stable is starts measuring again.

2.3.4 Air suction device, low air velocities

Comparable to the high-speed wind tunnel the low speed air pressure device characterises a screen material by generating a set number of air velocities through the screen and recording the resulting pressure difference over the screen. Earlier Miguel *et al.,* (1997, 1998) has developed an air suction device for typical characterisation of air pressure differences over screens a different low air velocities. For measurements of air permeability of screens at low velocities this air suction device is used. In order to create and accurately measure a very low air velocity a draining water tank is used where the draining water is controlled and measured instead of the air flow. Because this is a closed system except for this draining water and the air flow through the screen the volume flow of draining water equals the volume flow of air being sucked through the screen. The reason for using this set-up is because water flow can be measured much more easily and accurately then air flow.

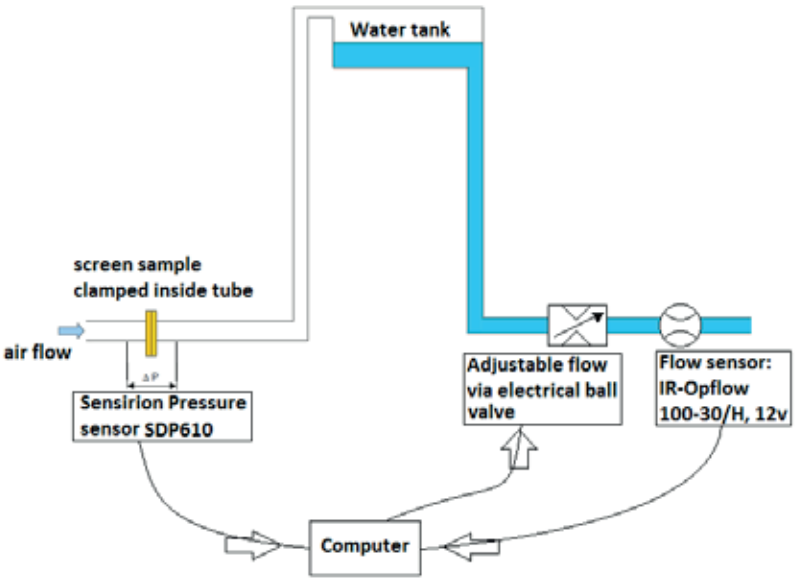

Figure 10 *Schematic overview of air permeability measurement set-up, the water tank is set up approximately 5 meters higher than the rest of the set-up.*

The flow sensor is manufactured by Tecflow International of the type Ir-Opflow 100-30/H with a stated accuracy of ±1%. The differential pressure sensor is produced by Sensirion of the type SDP610 with a stated accuracy of ±(0.2Pa + 3%). The data produced by the differential pressure sensor has to be corrected using the ambient pressure using the following formula:

$$dP_{eff} = dP_{Sensor} \cdot \frac{P_{Call}}{P_{ambiant}} = dP_{Sensor} \cdot \frac{966}{\sim 1013}$$

Where dP_{eff} is the corrected differential pressure, dP_{Sensor} is the sensor readout, P_{Call} is the ambient pressure at which the sensor was calibrated by the manufacturer and *Pambiant* is the ambient pressure at which the sensor is being used. For measurements carried out in Wageningen the atmospheric pressure recorded at weather station 'De Veenkampen' is used as a value for $P_{ambiant}$.

The height difference between the water tank and the rest of the set-up is necessary to create the required pressure difference over the screen sample (which is typically relatively low, the differential pressure sensor currently used has a range of 500 Pa while a water column of 5 m can generate roughly 50.000 Pa of pressure difference), the flow on the other hand is limited mainly by the flow sensor (an acoustical flow sensor would not have this same limitation). Another advantage of this height difference is that it reduces the pressure fluctuations caused by water movement inside the water tank relative to the total pressure difference.

2.3.5 Measurement procedure

Screen samples are prepared by attaching rings on both sides via a glue seal to ensure no air leaks out via the sides and to be able to place them in the set-up in a repeatable manner. For this task a glue applicator (type: Performus™ V, model nr: 7012334, equipped with gluing tips: Precision Tips GA GP .020X.25 PURPLE 50, from manufacturer: Nordson EFD) was used to apply a continues line of rubber sealant from Bison to metal rings type DIN 7603A 2.0 mm. 42 x 49 mm. Two rings are then placed on both sides of the screen sample and are cut out of the bulk screens after the rubber sealant has dried. Samples are placed in the air suction device.

During the measurement of a sample the following sequence is carried out by the system automatically:

1. Pressure sensor and flow sensor are set to record continuously.
2. Signal is send to the adjustable flow valve to increase the flow (action takes ~0.1 s).
3. Wait 0.5 s to stabilize the flow and pressure.
4. Pressure and flow data from the 2 seconds that follow are averaged and recorded as a measurement point
5. Return to step 1.
6. After repeating steps 1 to 4 ten times the measurement is complete and the adjustable flow valve is set to close.

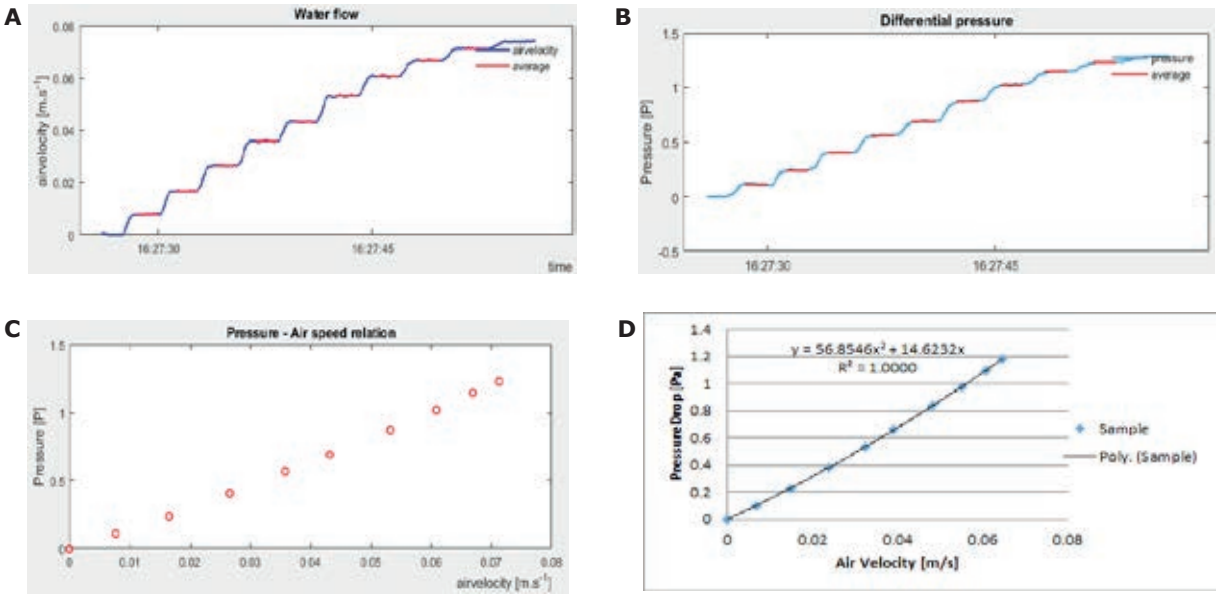

Figure 11 *Example measurement data showing a measurement cycle. A and B show complete time series of the flow and differential pressure data where the blue lines are the raw data logs and the overlaid red lines mark the data that is averaged to form the measurement points. C shows the air speed - pressure relationship for the characterised sample which is used to solve its permeability. D the same data as C in Excel.*

From the measurement sequence follows a pressure drop and air speed relationship, the Forchheimer-Darcy model is then fitted into this data and the permeability and inertial factor are solved using the coefficients. A detailed description of the fitting procedure and the resulting uncertainty's can be found in the appendix.

2.4 Measurement of humidity transport

2.4.1 Background

Greenhouse crops transpire water and are therefore a major source of humidity release to the air. Screens usually separate the warm and humid greenhouse volume from the cold and relatively drier roof volume. Water vapour transport through screens is a complex process resulting from different transport mechanisms:

- **Diffusion,** caused by the absolute humidity gradients at both sides of the screen, through pores of the material and the material itself.
- **Convection,** caused by the air movement generated by buoyancy (temperature gradients) and by wind (if greenhouse vents are open), through the pores of the material.
- **Absorption, transmission and desorption** of the water vapour by the fibres.

Diffusion (R) can be described by Fick's law

$$R = D * A * \frac{\Delta c}{d}$$

where R is the diffusion rate, D the diffusion coefficient or diffusivity A the surface area over which the diffusion occurs, d the distance over which the diffusion occurs and Δc the concentration difference between both sides (here different concentrations of absolute humidity).

Water vapour can diffuse through a screen in two ways: simple diffusion through the air spaces (macro and micropores) and along the plastic stripes and the fibres. In the case of hydrophilic fibre assemblies, water vapour diffusion does not obey Fick's law. It is governed by a non-Fickian, anomalous diffusion because adsorption, capillary flow and desorption play larger roles. The humidity diffusion through the air portion of the screen is almost instantaneous whereas through a fabric system it is limited by the rate at which humidity can diffuse into and out of the fibres or polymer, due to the lower humidity diffusivity of these materials.

Convection is a mode of mass transfer (here water vapour) that takes place while air is flowing through a material layer (here screen). The mass transfer in this process is controlled air movement generated by buoyancy (temperature gradients) and by wind (if greenhouse vents are open). The convective exchange is depending on air permeability of the material.

The sorption, transmission/migration and desorption process: A hygroscopic material absorbs water vapour from the close humid air and releases it in drier air. The amount of water vapour which can be absorbed by the materials is dependent on the fibre regain and the humidity of the atmosphere (%). This mechanism is relevant for screens, since conditions in greenhouse lead to possible condensation on the screens.

2.4.2 Cup method

2.4.2.1 Introduction

With the aim of characterizing humidity transport through the screens, exclusively caused by water vapour diffusion mechanisms, a set of seven heterogeneous screen samples were selected from the 29 screen samples provided by the companies (Figure 12). These samples were provided to the Laboratory of Postharvest Technology of Food & Biobased Research Institute of Wageningen University and Research, where water vapour transmission by diffusion for each sample was determined according to international norm ASTM E-96: Standard Test Methods for Water Vapour Transmission of Materials (also known as cup method).

Figure 12 *Screen samples selected for humidity transport measurements.*

2.4.2.2 Description of Cup method

In cup method, there is a gradient of absolute humidity maintained on two sides of the specimen, so that water has to diffuse through the specimen following the water vapour gradient. Parameters relating water vapour permeability are calculated after testing the water vapour transmission rate of the specimen under specified temperature and relative humidity. Cup method can be operated into two ways based on the same testing principle: desiccant method in which water vapour transmits into the test dish, and water method in which water vapour transmits out of the test dish.

In the water method (the method used in our measurements), the dish/cuvette contains distilled water, and the weighing determines the rate of water vapour movement through the specimen from the water to the controlled atmosphere. Figure 13 shows the testing principle of water method.

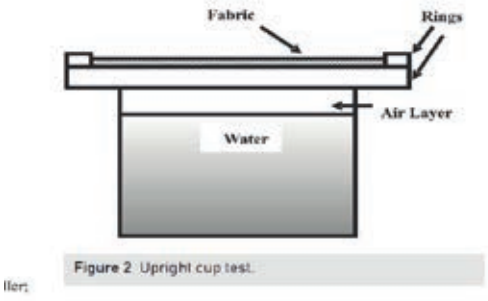

Figure 13 *Testing principle of upright cup water method.*

In the cup method, at least three assemblies are needed: test dish, testing environment and weighing appliance. The test dish/cuvette shall be of any non-corroding material, impermeable to water or water vapour. It may be of any shape. Lightweight is desirable. The easily folding or distorting specimen will need an external edge or frame at the open mouth of test dish for supporting. In our experiments, simple laboratory cuvettes were used. The test environment is realized in testing chamber. Its temperature should remain within + 1°C and humidity within + 2%. Air shall be continuously circulated throughout the chamber, with a velocity sufficient to maintain uniform conditions at all test locations. In general temperature is often controlled by single-heat because the testing temperature is always higher than lab temperature.

The air space between the distilled water and the specimen has a small water vapour resistance, but it is necessary in order to reduce the risk of water touching the specimen when the dish is handled. Such contact invalidates a test on hygroscopic materials. The cuvette is filled with water leaving a small air space between the water surface and the specimen. Then, the specimen must be sealed to the dish/cuvette (and clamping if desired, Figure 14) in such a way that the dish mouth defines the area of the specimen exposed to the water vapour pressure in the dish. The sealing of the edges of the specimen is important to prevent the passage of water vapour into, or out of, or around the specimen edges or any portion thereof.

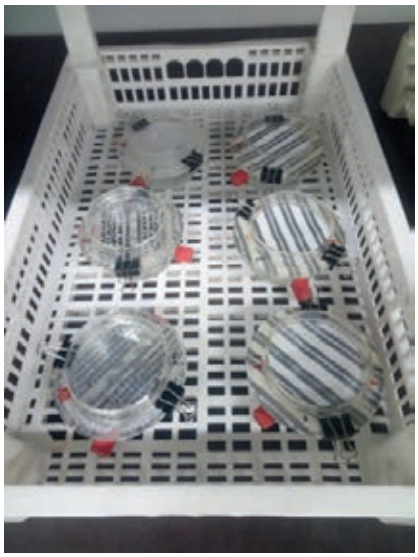

Figure 14 *Detail of the sealing of the specimens in the cuvettes using clamps.*

The dish assembly must then be weighed (a high precision analytical balance or other higher precision weighing appliance is needed enhancing the testing accuracy and shortening the testing period) and placed in the controlled chamber on a true horizontal surface. The test dish/cuvette is weighed periodically (Figure 15) until the rate of change is substantially constant.

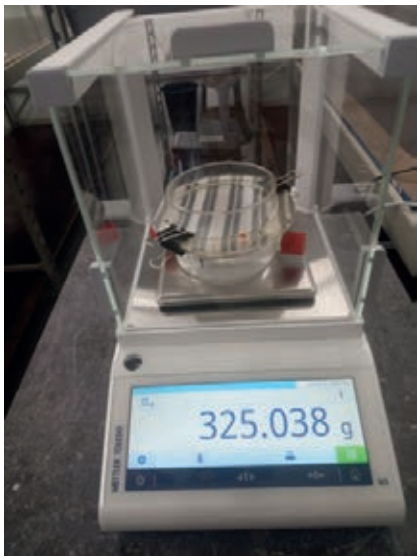

Figure 15 *Weighing operation of a cuvette with one of the specimens.*

The water vapour transmission (WVT) is then calculate as follows:

WVT=G/t*A

G = weight change (from the straight line) (g)
t = time (h)
G/t = slope of the straight line, (g/h)
A = test area (cup mouth area) (m^2)
WVT = rate of water vapour transmission ($g/h \cdot m^2$)

2.4.2.3 Description measurement conditions

The water vapour transmission rate (WVTR) is measured according to ASTM E96. Each screen sample was analysed in triplicate. Screen samples were clamped between the lid and the bottom of glass cuvette. The lid of the glass cuvette is open to assure the water vapour exchange through the samples. The exchange measurement area used for this test was 50 cm^2. A relative humidity of 100% is created inside the headspace of the cuvette. The cuvettes are placed during the complete duration of the test within environment where the temperature and the relative humidity are maintained to 19.4 ± 0.2°C and 60.7 ± 1.2% respectively.
Each cuvette is weighed few times during the experiment. The WVTR calculation is based on a linear regression of the weight loss versus time.

2.4.3 Swerea method

2.4.3.1 Introduction

One of the limitations of the cup method is that it only accounts with one of the three possible humidity transport mechanisms that can take place through a porous material (i.e. greenhouse screen), that is diffusion. However, in practice, greenhouse energy saving screens are located in greenhouses generating two different volumes, one below the screen, where the heating system and crop transpiration generate a warmer and more humid environment and one above the screen which is colder and dryer. This means that there is a temperature and water vapour gradient. On one hand this means that there will be airflow through the screen driven by natural or forced convection (depending on the opening of natural ventilation vents and on the presence of fans) depending on the air permeability of the screen. This convective airflow will also transport water vapour with it, which the cup method does not quantify. In addition, the temperature gradient on both sides of the screen will also lead to condensation on the inner part of the screen when screen temperature will be lower than dew point temperature. When condensation occurs, part of the water is transported through the screen and re-evaporated on the other side, accounting for an extra mechanism which is neither quantified by the cup method. As a consequence, a new measuring equipment and protocol should be used that accounts in a more realistic way for the conditions normally encountered in a greenhouse and which is able to quantify total humidity transport through greenhouse energy saving screens.
Swerea Insitute, Sweden, has developed and specific method (Swerea IVF 82-11) to perform these types of measurements.

2.4.3.2 Description of Swerea method

A specimen, in the form of a piece of greenhouse screen material, is placed as a barrier between two compartments having controlled climates. The climates at the two sides of the screen are fixed to conditions corresponding to those normally present at a real application in a greenhouse; one side with "warm and humid" air; the other side with "cold and dry" air (remark: humid and dry here refer to water vapour pressure). Due to a water vapour concentration difference in the air between the two sides water vapour will move from the humid side to the dry side. The amount of humidity passing through the specimen screen, having a known area, for a defined period of time and for the chosen climates, is measured. From these data, the flow of water vapour can be determined.

Measurement equipment main parts
The measurement equipment consists of the following main parts:

Climate chambers:	Allowing the temperature and relative humidity (RH) to be set at the desired levels generating "warm and humid" and "cold and dry" climates, respectively. The climate chambers include fans for circulating the air, and a built-in water container for the RH control.
Climate box:	Accommodated in the climate chamber generating "cold and dry" air but containing "warm and humid" air originating from the other climate chamber. It is made of five 5 cm thick plates glued together, leaving one side open. The plates consist mainly of an insulating material (expanded polystyrene), and being essentially impermeable to humidity. The outer cross-section measures 60 x 60 cm, and the height is 50 cm.
Connection pipes:	Allowing air to be circulated between the climate chamber generating "warm and humid" air, and the climate box.
Water level sensing devise:	Consisting of a laser based distance sensing device and a carburettor (floating plastic plate). The sensing device is connected to a data acquisition device logging the water level during the measuring period.
Specimen:	Consisting of a piece of greenhouse screen, 54 cm * 54 cm, provided with a "frame" consisting of duct tape. The surface of the screen not covered by tape measures 44 cm * 44 cm. The specimen is to be fixed over the open side of the climate box.
Reference weave	For calibration purpose a reference material (a certain type of weave) is used. By conducting reference measurements any small differences in measuring conditions between different measuring periods can be compensated for.
Tight PE-film	A PE-film, 0.2 mm thick, is used to perform measurements to detect any leakage in the system. In this context, the PE-film is considered completely vapour tight. Therefore, any indicated "humidity flow" is an indication of a (usually small) leakage in the system, which can be compensated for. (Comment: this value is normally close to 0 g/m^2/h).

Measurement equipment set-up
The climate box is placed in the climate chamber generating "cold and dry" air. One of the walls of the box is provided with two holes on which two connection pipes are fixed. The pipes lead to the interior of the climate chamber generating "warm and humid" air, through holes in the walls of the chambers. One of the pipes are connected to the air circulation system of that climate chamber, creating an air flow in that pipe. Hence, the climate in the climate box is to a large extent controlled by the climate in the climate chamber generating "warm and humid" air. This arrangement creates two different climates, with respect to temperature and RH, at the two sides of the specimen screen.

The water level sensing device is placed in the water container which is integrated in the climate chamber generating "cold and dry" air. Any extra humidity passing through the specimen will eventually condensate on the surface of the water in that container and thereby affecting the level of that water surface. Hence, the rate at which that water surface is rising is thereby a measure of the humidity flow through the specimen screen.

Principal sketches of the measurement equipment are shown in Figure 16 and Figure 17.

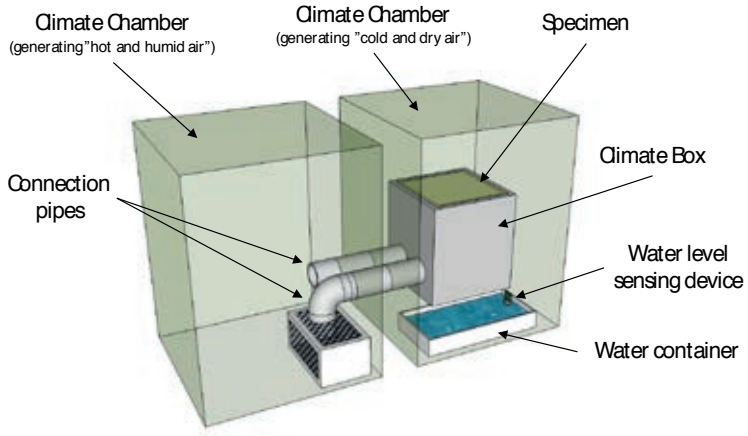

Figure 16 *Principal sketch showing the main parts of the measurement equipment.*

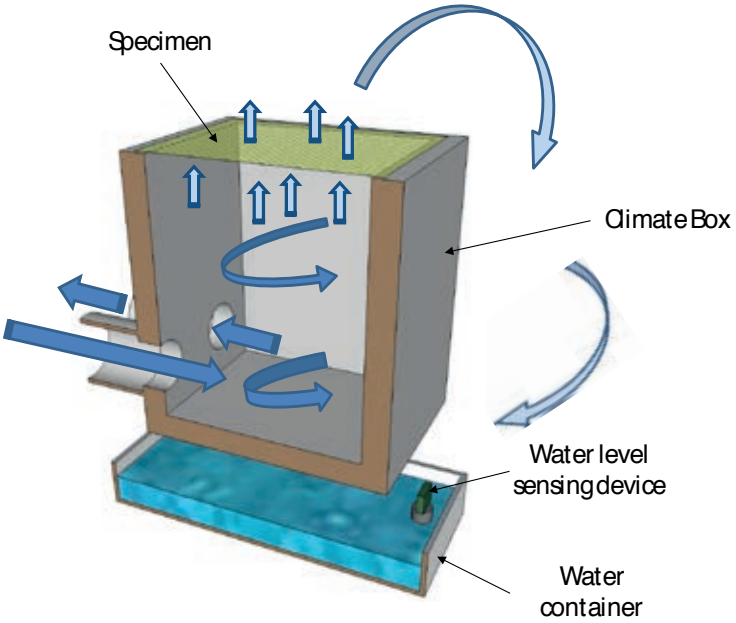

Figure 17 *Sketch of the cross-section of the climate box principally showing the path of air flow (dark blue arrows) and humidity transport (light blue arrows).*

2.4.3.3 Description measurement conditions

The air speed below and above the specimen are approximately 0.1 and 0.75 m/s respectively. The temperature and humidity in the chamber generating "warm and humid" air is set to 20°C and 80% RH, and the corresponding values in the chamber generating "cold and dry" air is set to 10°C and 80% RH.

2.4.3.4 Measurement procedure

Number of specimen

For each greenhouse screen material to be tested not less than 3 specimens shall be prepared, unless otherwise agreed.

Reference weave and tight PE-film

Measurements using the reference weave and the tight PE-film shall be conducted at least at two occasions: at the beginning of the measuring series and at the end.

A measurement –step by step

A measurement of the water vapour flow through a specimen consists of the following steps.

1. the open side of the climate box is covered with a prepared specimen using tape to seal all four sides of the specimen.
2. The climate chambers are set to the correct climates.
3. The water level device is activated for data acquisition.
4. The specimen and measuring equipment is then left for steady state flow to establish and for water level data to be collected.
5. The duration of one measurement shall be at least 16 hours.
6. The humidity flow is determined from the slope of the water level-time curve (generally a straight line) which is formed during the measurement.

Calculations and expression of results

The primary water vapour flow, Fp (g/m²/h), is calculated using the following formula:

$$F_p = \frac{\Delta z A_{wc} \rho_w t_{s,1h}}{t_s A_s}$$

where:

F_p	=	*Humidity flow through the specimen at the present measuring conditions*	[g/(m² h)]
Δz	=	*Level change of water surface during measuring period*	(mm)
A_{wc}	=	*Area of the cross-section in the horizontal plane of the water container*	(mm²).
$t_{s,1h}$	=	*Number of seconds per hours*	
t_s	=	*Number of seconds of the measuring period*	
A_s	=	*Area of the uncovered specimen*	(m²)
ρw	=	*The density of water*	(g/mm³)

To compensate for any small inevitable differences in measuring conditions originating from the measuring equipment, measurements are conducted on the tight PE-film and reference weave, and the primary value of the water vapour flow adjusted using the following equation.

$$F_s = (F_p - F_{PE}) \cdot \frac{F_{R,d}}{F_{R,a} - F_{PE}}$$

where

F_s	=	*Water vapour flow through the specimen, adjusted value.*	*[g/(m² h)]*
F_p	=	*Measured primary value of the water vapour flow*	*[g/(m² h)]*
F_{PE}	=	*Average value for the tight PE-film prior to and after the measurement on the current specimen (normally negligible)*	*[g/(m² h)]*
$F_{R,d}$	=	*74.4 (defined water vapour flow value of the reference weave)*	*[g/(m² h)]*
$F_{R,a}$	=	*Average value for the reference weave prior to and after the measurement on the current specimen*	*[g/(m² h)]*

2.5 Model for overall energy saving of materials

2.5.1 General description of energy model KASPRO

The greenhouse process (KASPRO) model is a dynamic model for calculating greenhouse climate and energy consumption. The model is constructed from modules describing the physics of mass and energy transport in the greenhouse enclosure, and a large number of modules that simulate the customary greenhouse climate controllers. Thus, the model takes full account of mutual dependencies between greenhouse characteristics and its climate control. The state variables and boundary conditions in the KASPRO model are shown in Figure 18. Full details of the model can be found in "Analysing energy-saving options in greenhouse cultivation using a simulation model" (de Zwart, 1996).
The simulation of the greenhouse physical processes comprises the energy and mass fluxes in the enclosure. These fluxes result in a transient course of temperature, humidity and CO_2 concentration.
All processes are parameterized according to their physical characteristics like optical parameters in the visible and infrared wavelengths, their inertia and physical limitations (*e.g.* maximum ventilation capacities, leakage, maximum heating or cooling power etc.).
The climate controller of the KASPRO simulation model mimics the behaviour of commercial greenhouse climate computers controlling by means of heating, cooling, ventilation, dehumidification, misting, shading, artificial illumination, and carbon dioxide supply. The model also describes the behaviour of the boiler, short-term and seasonal heat storage facilities, co-generation of heat and electricity and heat pumps.
The interface with these controllers is similar to the interface that growers are familiar with; the definition of time-varying setpoints for heating, ventilation, dehumidification and CO_2-supply.
The inner climate in terms of PAR-radiation and temperature results in crop biomass production according to the well-known photosynthesis models (Goudriaan and van Laar, 1994). Periods of unfavourable temperatures are taken into account, resulting in a decrement of actual photosynthesis in comparison to maximal photosynthesis under the given light and CO_2-conditions.
The model has shown to be helpful in understanding the phenomena observed in greenhouses and has a high predictive value for the energy consumption, inside humidity and temperature conditions under given outside climate conditions and greenhouse parameters.

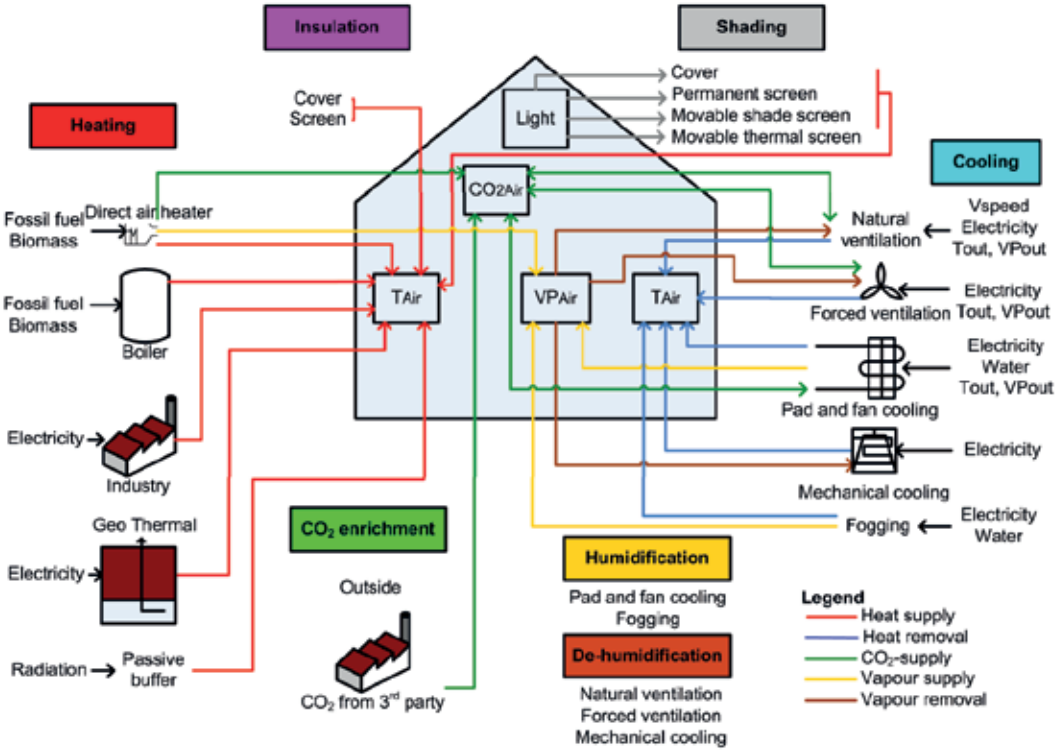

Figure 18 *Schematic overview of greenhouse energy model.*

2.5.2 Energy balance of an energy saving screen

The energy fluxes through a screen in a greenhouse can be described by Figure 19.

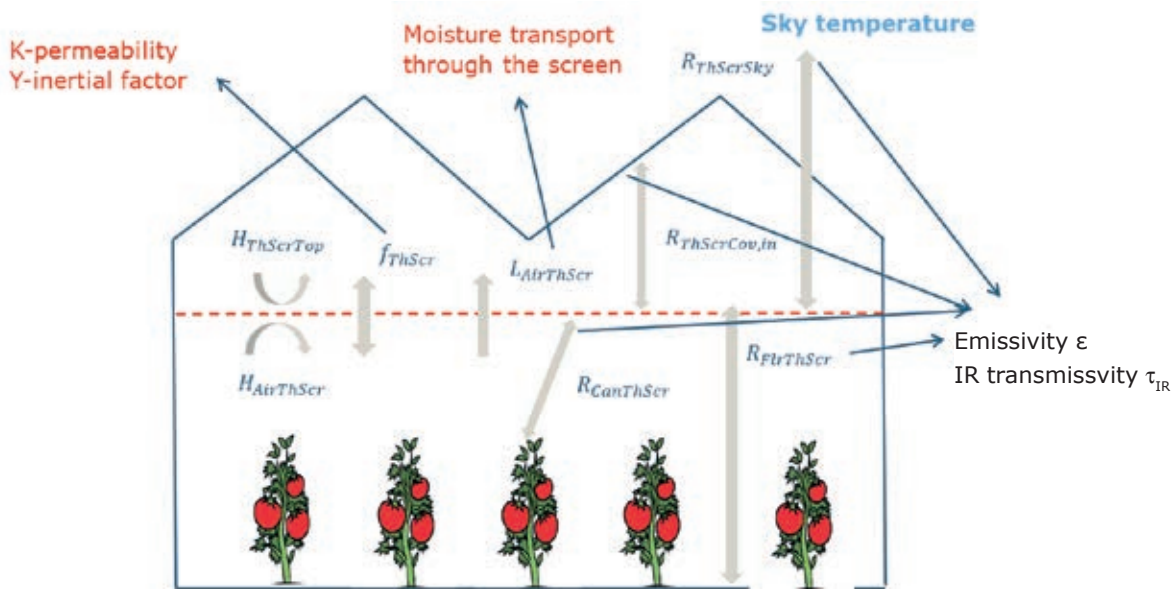

Figure 19 *Detail of the energy fluxes around a deployed single thermal screen in a greenhouse.*

In KASPRO, the state variables of the model are all described by differential equations. The derivatives of the state variables to time are indicated by a dot above the state symbol.
Temperature of the thermal screen TThScr is described by:

$$cap_{ThScr}\dot{T}_{ThScr} = H_{AirThScr} + f_{ThScr} + L_{AirThScr} + R_{CanThScr} + R_{FlrThScr} + R_{PipeThScr} - H_{ThScrTop} - R_{ThScrCov,in} - R_{ThScrSky}$$

where *capThScr* is the heat capacity of the thermal screen; $L_{AirThScr}$ the latent heat flux caused by different mechanisms of humidity transport through the screen; $R_{PipeThScr}$, $R_{ThScrCov,in}$ and $R_{ThScrSky}$ the thermal infrared radiation fluxes between the heating pipes and the thermal screen, the screen and the internal greenhouse cover layer and the screen and the sky, respectively; $H_{AirThScr}$ and $H_{ThScrTop}$ the heat exchange (convection) of the air to the screen low layer and the screen top layer to the roof compartment air and f_{ThScr} the sensible heat flux through the screen caused by the temperature difference on both sides of the screen.

KASPRO quantifies the energy balance of the screen estimating all energy fluxes previously shown.
For the sensible heat transport through the screen, the equation for buoyancy driven air flow through porous media was used, combined with Darcy's law, making the amount of air flow through the screen dependent of the permeability of each screen and the absolute value of the temperature gradient on both sides of the screen. So, for example, when using a single screen, the heat exchange from air to top through the screen can be computed by:

$H_{AirTop} = 2.3e^{3} * (T_{air} - T_{top}) * k * 1200 * (T_{air} - T_{top})$ [W/m²]

The permeability k relates an air exchange to a pressure difference and the term $2.3e^{3}$ in the formula is the factor that translates a temperature difference to such a pressure difference.

Finally, the radiative exchanges can be calculated using the Stefan-Boltzman law, using the emissivity values of each screen. The general description of radiative heat transfer is:

$$R_{S1S2} = \frac{\varepsilon_{S1}\,\varepsilon_{S2}\,F_{S1S2}\,A_{S1}}{1-r_{S1}r_{S2}F_{S1S2}F_{S2S1}}\,\sigma\,(T_{S1}^{4} - T_{S2}^{4}) \quad [W]$$

This equation, computing the energy exchanged from surface S1 to surface S2, is governed by the thermal radiative material properties of both surfaces and the geometrical configuration. The material properties are described by the emissivities (ε_{S1} and ε_{S2}) and the infrared reflection coefficients (r_{S1} and r_{S2}). The geometrical configuration is defined by the radiation surface (A_{S1}) and the viewfactor, a number between 0 and 1 which gives the fraction of the hemisphere of the radiating surface that is occupied by the surface S2. σ is the constant of Stefan-Boltzman ($5.67e^{-8}$ W/K⁴). The nominator of this equation describes the primary radiative exchange between surface S1 and surface S2. The denominator takes account for the diminishing of the net radiation due to re-radiation by reflectivity of the destination surface. Obviously, when the reflection coefficient of one of the surfaces is zero, the denominator becomes 1 and re-radiation does not play a role. When, however, the reflectivity of a surface is large, for example when using aluminized energy screens, re-radiation gives an important diminishing of the net radiative exchange. For this re-radiation, not only the viewfactor of surface S1 to surface S2 plays a role, but also the viewfactor from surface S2 to surface S1 (so telling how much of the hemisphere of S2 is occupied by S1).

For the latent heat transport, KASPRO estimates the amount of water vapour transported through the screen accounting only for the two most important of the three basic humidity transport mechanisms for the majority of the screens: convection (dependent on the air permeability of the screen) and condensation-transmission-re-evaporation, whereas diffusion is not directly modelled.
The equation that KASPRO uses to model the flow of air through the screen that is used to calculate moisture transmission through screens is the following:

air flow=sc*2300*k*fabs(dt)+(1-sc)*0.02*fabs(dt)+l [m³/s/m²)

Where *sc* is the screen opening/closing (being 0 screen completely open and 1 screen completely closed), *2300*

the the factor that translates a temperature difference to a pressure difference, *k* the screen permeability (m^2), *fabs(dt)* the absolute value of the temperature gradient across both sides of the screen, 0.02 an empirical parameter to calculate airflow through the gaps when screen is not fully closed and *l* an air leakage which is present even if the screen is virtually impermeable and is fully closed ($l=0.0005\ m^3/s/m^2$).

2.5.3 Description of calculation assumptions

In order to quantify the energy saving of the screens, a realistic simulation of a typical tomato crop growing cycle following Het Nieuwe Telen has been carried out. In order to account for a very representative outside climate, a typical meteorological year (SEL2000), which was built using a large number of yearly weather datasets for a location (de Bilt) in The Netherlands, has been used as input. This section contains a detailed description of the greenhouse (size, covering material, etc.), equipment (heating system, screen, etc.) and all the set points used for the simulation.
A first simulation has been performed in which no screen was used, which constitutes the reference case. Then, maintaining all the settings, simulations have been performed for each one of the 7 selected screens. Earlier measured screen properties of those 7 screens are available. In order to perform simulations which are as representative as possible to commercial growers practice, all settings and basic principles of Het Nieuwe Telen have been used, except for some simplifications that have been adopted: energy saving screens are only used during night-time period (no daylight use); when used, energy saving screens are always completely closed (no gaps); no artificial-lights.

Table 1 shows the simulated crop details.

Table 1
Crop and cropping period.

Crop:	tomato
Transplant date:	15-12
End of crop cycle:	20-11

Table 2 shows the most important parameters considered in the simulations concerning the greenhouse and its cover.

Table 2
Greenhouse system

Greenhouse construction		
Area:	40,000	m^2
Path width:	5	m
Gutter height:	7	m
Roof slope:	22	degree
Span width:	4	m
Section size:	5	m
Cover:	Standard glass	
Leakage:	7.50E-05	$m^3/(m^2\ s)/(m/s)$
Window length:	1.67	m
Window height:	1.5	m

Table 3 shows the essential details of the simulated heated system.

Table 3
Heating system

Heating system	
Primary heating network:	Low
Low pipes diameter:	51-er
Number low heating pipes per span:	5
Top pipes diameter:	32-er
Number of top heating pipes per span:	2.5
Boiler power:	200 W/m^2
Hot water buffer volume:	200 m^3/ha

Table 4 shows the essential details on the screen configuration and set points used for the simulations.

Table 4

Screening setpoints.

Screen system:		Energy screen
Screen type[1]:	Date	Setpoint
Max T_{out} screen[2]:	13-11	14°C
"	16-2	12°C
"	01-6	10°C
"	1-10	12°C
Screen close below[3]:		5 W/m^2
Chink on temperature Excess[4]:		0 %
Chink On humidity excess[5]:		0 %

1 The name of the screen is written here. Kaspro then reads screen properties from a .txt file in which all screen properties have been written.

2 When external temperature is above this value, the screen is not used

3 Screen is used whenever external solar radiation is below this value

4 Percentage of gap opening of the screen when temperature exceeds the set point

5 Percentage of gap opening of the screen when humidity exceeds the set point

Table 5 shows the most important set points used in the simulations.

Table 5

Temperature setpoints for heating and ventilation, humidity and CO_2 setpoints.

Set points	Date	
	Date	Setpoint
Heating temperature (°C):	15-12	19
"	26-12	21 17 17.5
"	16-1	23 23 16 19
"	16-2	21 21 14 17
"	20-4	20.5 20.5 14 16.5
"	26-6	19.8 19.8 14 17.5
"	10-9	20 14 17 17
"	13-11	20
Dead zone (°C)[1]:	15-12	4
"	1-3	3
"	1-4	2
Relative humidity (%):		90
CO_2(ppm):		700
CO_2 dosing rate (kg/ha/h):		120

1 Ventilation temperature set point is heating set point plus this value

3 Results

3.1 Radiative exchanges through screens

3.1.1 Measurement protocol Emissivity measurement device

A measurement protocol for the emissivity measurement device has to be established in order to reach maximum possible repeatability and to minimize measurement errors. No data is provided by TNO on the margin errors of the emissivity measurement device. In order to investigate the overall variations in measurements during different sessions, we have measured the emissivity, IR transmissivity and IR reflectivity of an ETFE film in between all other measurements during different sessions. In order to have a stable and reliable measurement, it is recommended to use a sample with a known emissivity value as reference material.
Each time when the emissivity value of ETFE film was deviating too much from the expected value, we have repeated the calibration (2.2.3). According to our observations, the more variations in the climate conditions of surrounding area, the more often new calibrations are needed. The results of measurements of ETFE film during 2 different sessions are shown in the Table 6 and Figure 20. Each session consists of 5 measurements/trials.

Table 6
Thermal properties of ETFE measured with the emissivity measurement device.

ETFE	IR reflectivity r_{IR}	IR transmissivity τ_{IR}	Emissivity ε
Trial 1	14	29	57
Trial 2	17	31	52
Trial 3	16	31	52
Trial 4	15	29	56
Trial 5	15	30	56
Trial 6	17	33	50
Trial 7	16	32	52
Trial 8	17	31	53
Trial 9	16	29	55
Trial 10	15	29	56

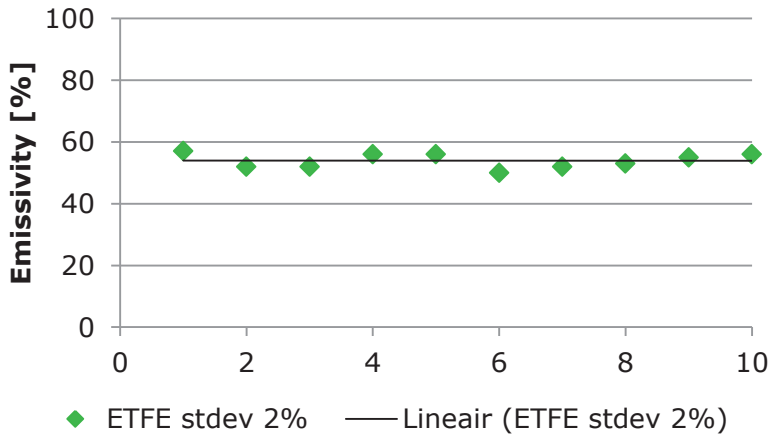

Figure 20 *Emissivity of ETFE measured with the emissivity measurement device.*

The obtained standard deviation of repeated measurement of ETFE for both sets of measurements is about 2%, which also is the same for the set of 10 measurements in total. It is important to notice that ETFE film is a homogeneous sample and displacement of this sample has no effect on the measurements. In practice, many of energy screens are a combination of different materials with different patterns which may affect the measurements results.

3.1.2 Measurement results screen materials

The emissivity of the 7 selected samples is measured according to the procedure described in a previous section. The results of these measurements are presented in Table 7.

Table 7

Emissivity of 7 selected screen samples.

Screen	Average Emissivity ε	stdev (%)	Average Transmissivity τ_{IR}	Average Reflectivity r_{IR}
BP16A	2.4	2	73.8	23.4
LS16U	46.8	2	33.4	20.0
CU16O	54.4	5	28.2	17.4
NT16D	9.6	2	23.0	67.6
NT16H	67.0	0	9.4	23.6
NT16K	32.0	3	49.8	18.2
NT16M	77.6	3	7.2	15.0

We can observe that screens BP16A and NT16D have the lowest emissivity. Table 7 further shows that screens NT16M, NT16H and also NT16D and CU16O show a low IR transmissivity. Only NT16D shows a combination of low emissivity and low IR transmissivity, resulting in a high IR reflectivity.

The measurements are carried out on different days. As mentioned before, the structure and pattern of the sample might affect the measurement results. The results of 5 measurements on each selected sample are shown in Figure 21. Typical variations in screens while displacing the sample during each measurement result in a standard deviation in emissivity of 2-3%, a little higher than for ETFE. Only sample CU16O shows a higher standard deviation in emissivity (5%), which can be explained by inhomogeneity in its thickness. The thinner the sample, the less heat will be absorbed, which will result in a lower radiative emittance.

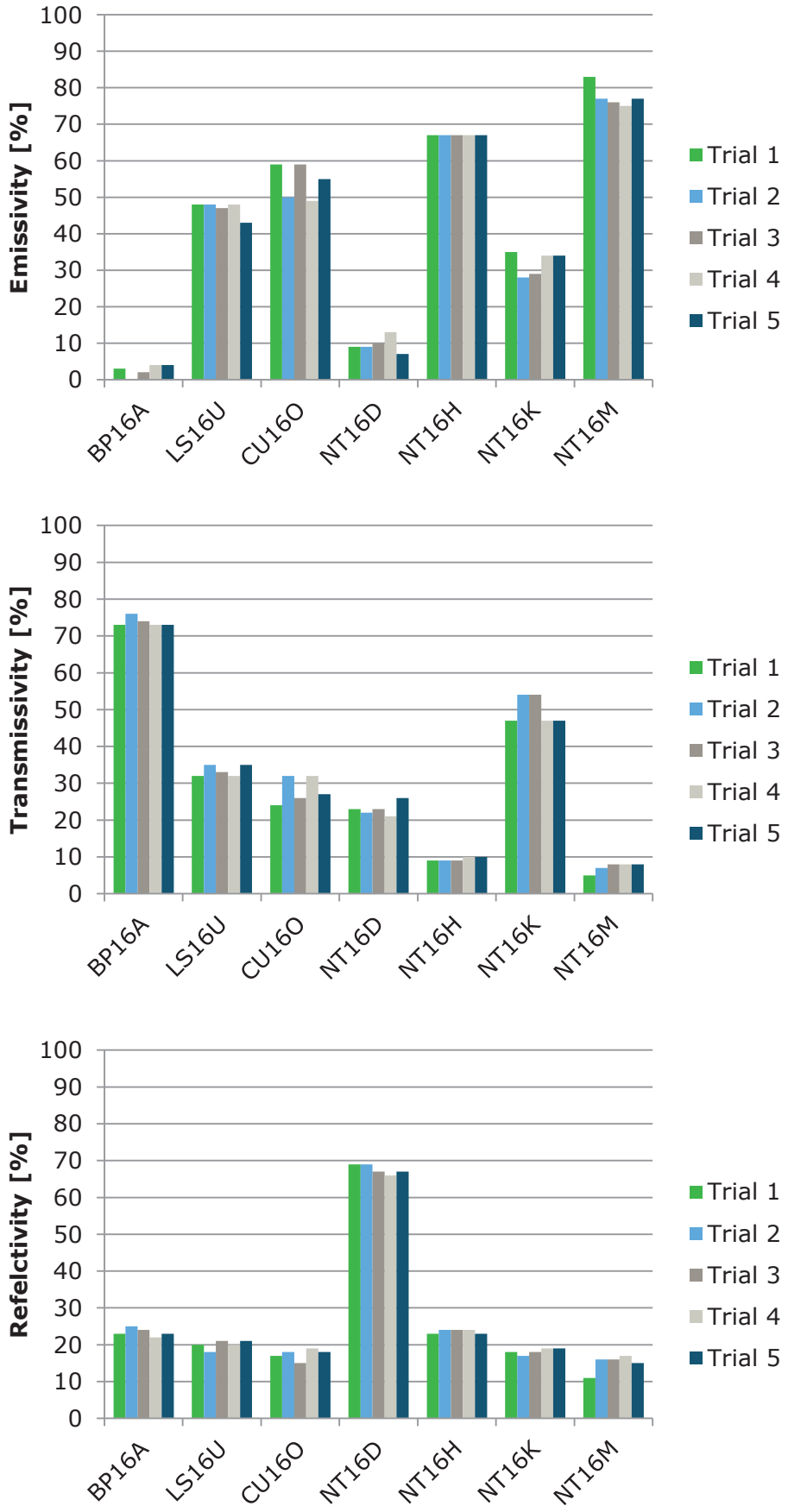

Figure 21 *Emissivity of 7 selected screen samples, 5 measurements per sample.*

Some of energy screens are aluminized on one side. For these samples the measurements must be done on both sides, especially if multiple screens are used. We selected 3 one-sided aluminized screens (NT16D, NT16E and NT16F) with different percentages of porosity and almost the same percentage of aluminum in it. Samples NT16E and NT16F are porous samples with the same fabric on the backside. Sample NT16D is completely non-porous and has a (plastic) laminated backside. The results of these measurements are presented in Figure 22. The sample codes indicated with _180 present the measured values on the backside of screen.

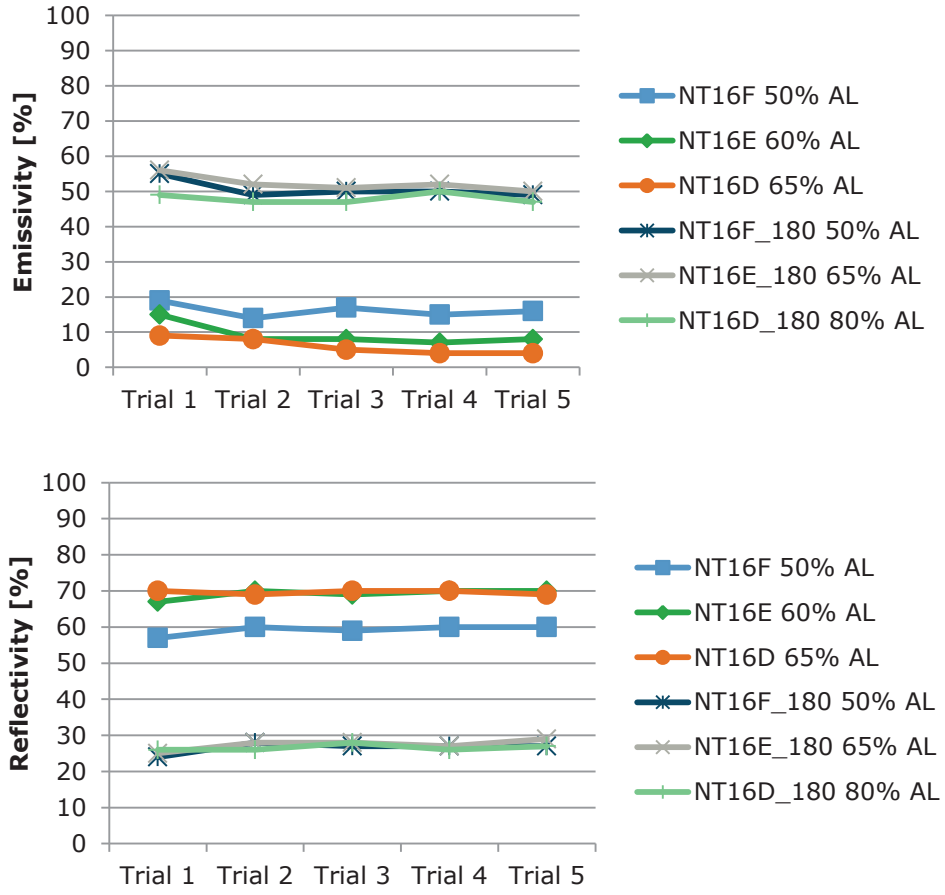

Figure 22 *Emissivity and IR reflectivity of both sides of 3 aluminized screen samples.*

The measurement results of these 3 samples show a significant difference in heat emitting performance of both sides. The main difference is caused by differences in reflectivity (Figure 22). Another interesting conclusion is that the emissivity value of all 3 samples are about the same, regardless of porosity or type of backside fabric/ film.

3.2 Air permeability of screens

3.2.1 Results air velocity measurements in greenhouses

In order to determine the air velocities in a greenhouse with and without natural ventilation, measurements have been carried out using 3D anemometer sensors. Figure 23, Figure 24 and Figure 25 show the values of the vertical component of the air velocity vector in the XY plane for the three sensors, respectively, together with the external wind velocity values (m/s, divided by 10 for convenience to fit them in the same scale as the rest of parameters), the opening of leeward and windward roof vents (in a 0-1 range, being 0 vents fully closed and 1 vents fully open) and the closing of both the shading and the energy saving/black-out screen (in a 0-1 range, being 0 vents fully closed and 1 vents fully open) for the 25 September 2016.

From Figure 23 we can highlight that during the daytime period, when both screens are not used and vents are open more than 50%, the measured air velocity values are higher, as might be expected. The values measured in the top sensor are consistently higher than those measured in the middle sensor, and those in the middle sensor higher than those in the lower sensor. This suggests that the vent above the sensors is acting as an inlet and therefore, values of the sensor near the vent are the highest with air velocity decreasing as the air flow penetrates lower in the greenhouse.

On the other hand, during the night time period, when both screens are used and roof vents are open on a lower percentage, the vertical component of air velocity values are much lower than during the daytime period, as might be expected.

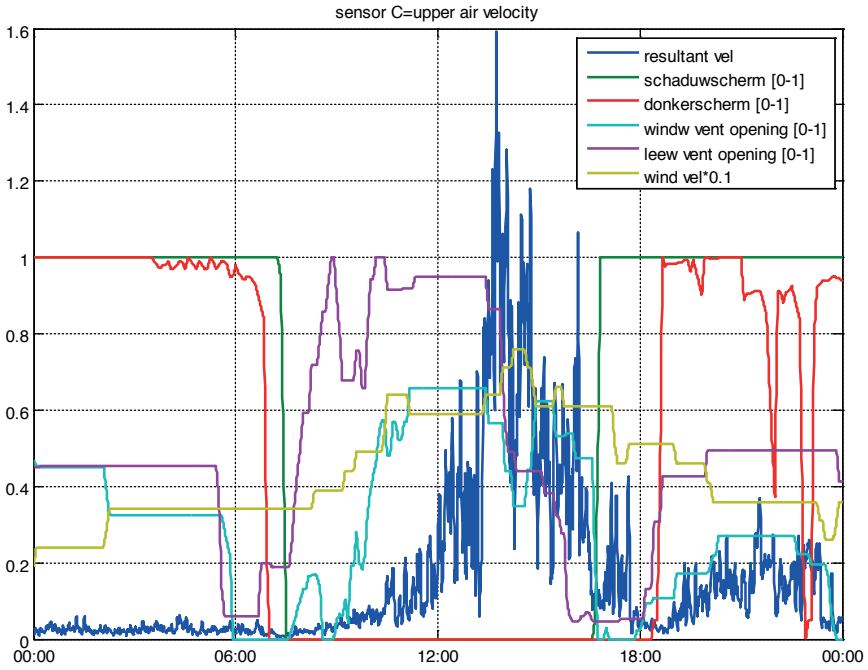

Figure 23 *Vertical component of air velocity vector on the top sensor (R_A), external wind velocity (10% of the value), position of leeward and windward greenhouse vents (0-1) and position of shading and energy saving/ darkening screens (0-1) for day 25 September 2016.*

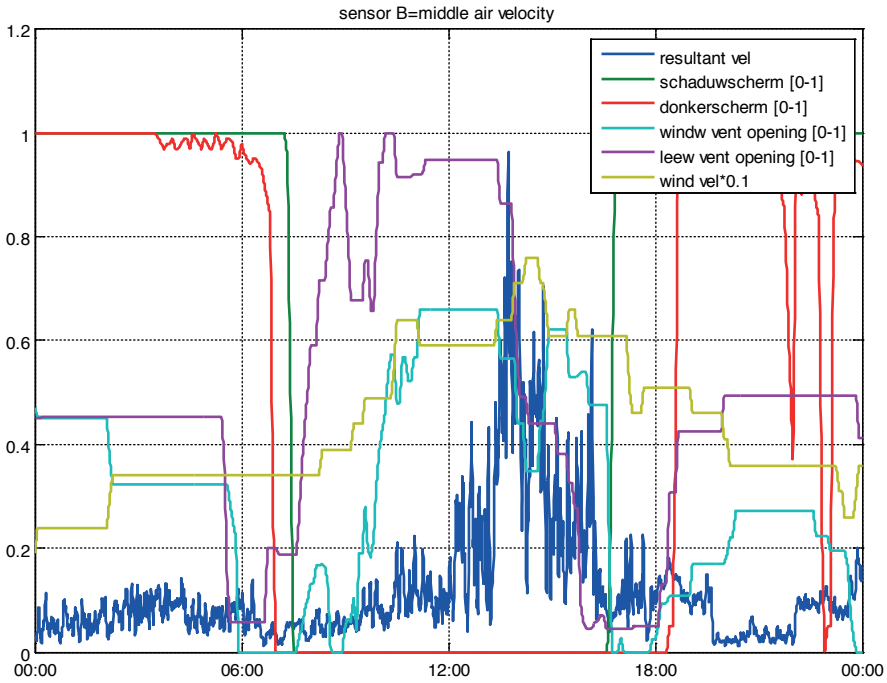

Figure 24 *Vertical component of air velocity vector on the middle sensor (R_B), external wind velocity (10% of the value), position of leeward and windward greenhouse vents (0-1) and position of shading and energy saving/darkening screens (0-1) for day 25 September 2016.*

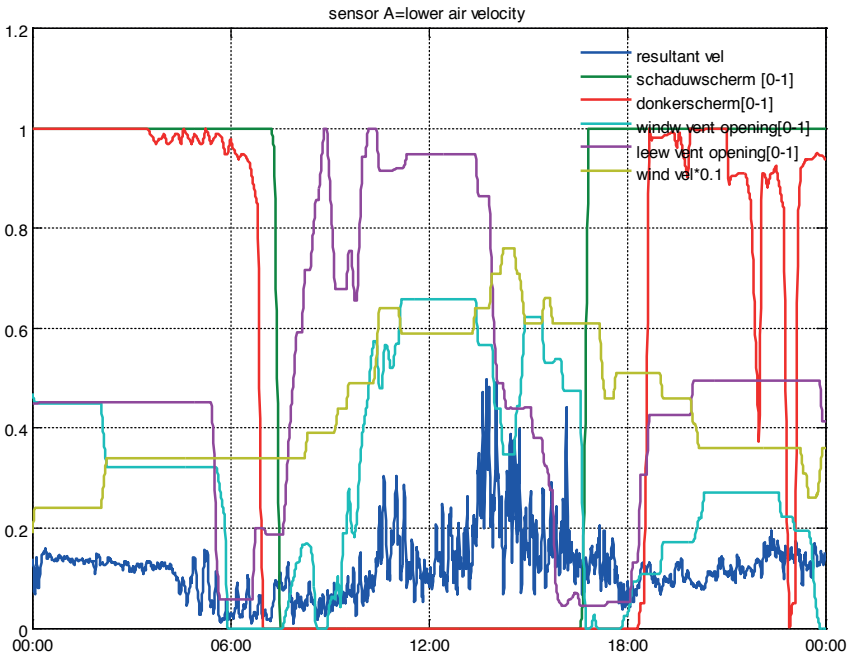

Figure 25 *Vertical component of air velocity vector on the lower sensor (R_C), external wind velocity (10% of the value), position of leeward and windward greenhouse vents (0-1) and position of shading and energy saving/darkening screens (0-1) for day 25 September 2016.*

In order to better understand the interaction between the opening and closing of the roof vents and the screens, as well as the external wind speed, with the values of the vertical component of air velocity measured by the 3 sensors, the measurement period has been divided into different scenarios.

Roof vents open more than 50%-Screens not used (0)-Wind velocity>0.5 m/s

Table 8 shows the mean and maximum values of the vertical component of air velocity measured in the three sensors (A, B and C) as well as for the normalized air velocities for exterior wind velocities higher than 0.5 m/s.

Table 8

Mean and maximum values of air velocities measured in greenhouses without screens for outside wind velocity >0.5 m/s and roof vents >50% open.

	Mean / max. vertical component of air velocity	Mean /max. normalized air velocity
Top Sensor (C)	0.18 / 1.77	0.05 / 0.61
Middle sensor (B)	0.15 / 1.09	0.05 / 0.45
Lower sensor (A)	0.14 / 0.7	0.05 / 0.39

This table shows that when vents are largely open and screens are not used, air velocity values near the vents can be higher than 1 m/s, for the measured position and for a greenhouse without insect proof screen on the vents. It also shows that for the measured position, air velocity decreases gradually from the top sensor, nearest to the vent to the lower sensor, furthest from the vent. This may suggest that the specific vent where measurements were made could act as an inlet most of the time, but that should be verified analysing the vector direction, which is not relevant for this present work.

Roof vents open between 1-50%-Screens not used (0)-Wind velocity>0.5 m/s.

Table 9

Mean and maximum values of air velocities measured in greenhouses without screens for outside wind velocity >0.5 m/s and roof vents >50% open.

	Mean / max. vertical component of air velocity	Mean / max. normalized air velocity
Top Sensor (C)	0.13 / 1.4	0.03 / 0.26
Middle sensor (B)	0.11 / 0.86	0.03 / 0.24
Lower sensor (A)	0.10 / 0.5	0.03 / 0.26

If roof vents are less open, results show that the decrease in the values of the vertical component of air velocity is lower than measured for a larger % of vent opening. With vents open to a lower percentage, the values of normalized air velocity are more stable for the different heights. When the vent is closing, airflow may change and become more horizontal, penetrating less towards the canopy.

Roof vents open more than 50%-Shading screen closed more than 80%-Energy saving screen not closed (0)-Wind velocity>0.5 m/s.

Table 10

Mean and maximum values of air velocities measured in greenhouses with closed shading screens for outside wind velocity >0.5 m/s and roof vents >50% open.

	Mean / max. vertical component of air velocity	Mean / max. normalized air velocity
Top Sensor (C)	0.13 / 0.38	0.03 / 0.08
Middle sensor (B)	0.15 / 0.4	0.03 / 0.1
Lower sensor (A)	0.17 / 0.5	0.04 / 0.12

The presence of the shading screen when vents are largely open changes the vertical profile observed compared to the situation without a screen. In this case, the air velocity values measured by the sensors below the screen are larger than those measured above the screen, which suggests an upward flow towards the vent, which may be acting in this case as an outvent. It also shows that when shading screens are used and vents are largely open, air velocity near the screens can be as high as 0.4 m/s in locations directly under the vents (this velocity being probably lower in locations which are not exactly below the roof vents).

Roof vents open less than 50%-Shading screen closed more than 80%-Energy saving screen not closed (0)-Wind velocity>0.5 m/s.

Table 11

Mean and maximum values of air velocities measured in greenhouses with closed shading screens for outside wind velocity >0.5 m/s and roof vents >50% open.

	Mean / max. vertical component of air velocity	Mean / max. normalized air velocity
Top Sensor (C)	0.08 / 0.9	0.02 / 0.18
Middle sensor (B)	0.06 / 0.54	0.01 / 0.11
Lower sensor (A)	0.07 / 0.27	0.02 / 0.3

If screens are opened to a lesser extent, then both mean and maximum values measured at the three positions are lower than those measured when vents are open to a larger extent. It also shows that the presence of the shading screen induces a decrease in the air velocity values, unlike when vents were more open. This could be due to the fact that if vents are more closed, the airflow pattern near the vents may be different from that observed if they are more open. However, this is not the objective of the study, which is more focused on knowing the absolute values of air velocity near the screens under different scenarios. In this sense, it is interesting to know the % of time that air velocity near the closed screen is higher than 0.1 m s^{-1}. For sensors C and B, located above and below the shading screen, this time percentage is 24.6% and 12.2%, respectively. If we analyse the moments in which the values are higher than 0.2 m s^{-1}, it only represents 6% of the time for sensor C and 2.6% of the time for sensor B.

Roof vents open less than 50%-Shading screen not used (0)-Energy saving screen closed more than 80%-Wind velocity>0.5 m/s

Table 12

Mean and maximum values of air velocities measured in greenhouses with closed energy screens for outside wind velocity >0.5 m/s and roof vents >50% open.

	Mean / max. vertical component of air velocity	Mean / max. normalized air velocity
Top Sensor (C)	0.06 / 0.25	0.02 / 0.07
Middle sensor (B)	0.07 / 0.18	0.03 / 0.14
Lower sensor (A)	0.08 / 0.18	0.04 / 0.25

In this scenario, we can observe an important decrease in both the mean and maximum values of air velocity. Mean values are lower than 0.1 m s^{-1} in sensors A and B which are located both below and above the energy saving screen. In general, the vertical air velocity profile suggests that air is moving upwards from the crop area due to natural convection, generated by the heating system, and the presence of the screen decreases this air velocity values. The higher peak values on the upper sensor could be a result of incoming airflow from the vents, when they are not fully closed. The amount of time for this scenario in which air velocity values measured by the sensors located below and above the energy saving screen (A and B) were higher than 0.1 m s^{-1} was 16.4% and 10%, respectively, and values during the measured period sensors never peaked above 0.2 m s^{-1}, as we can see in Table 12.

Roof vents open less than 50%-Shading screen closed more than 80%-Energy saving screen closed more than 80%-Wind velocity>0.5 m/s.

Table 13

Mean and maximum values of air velocities measured in greenhouses with closed energy screens for outside wind velocity >0.5 m/s and roof vents >50% open.

	Mean / max. vertical component of air velocity	Mean / max. normalized air velocity
Top Sensor (C)	0.06 / 0.6	0.02 / 0.32
Middle sensor (B)	0.04 / 0.36	0.01 / 0.37
Lower sensor (A)	0.07 / 0.25	0.02 / 0.3

In this scenario, with both screens used, we can observe that the lowest mean values are obtained in the sensor located between the two screens, which makes sense as this is the most confined sensor, being the upper sensor closer to the vent, and thus, with more influence from the inflows and outflows and the lower sensor being more affected by air moving upwards by buoyancy from the heating system. In this scenario, the % of time that the air velocity values are higher than 0.1 m s^{-1} for the three sensors (A, B and C) is 20.4%, 9.24% and 18.75% respectively, and for values higher than 0.2 m s^{-1} is 0.06%, 0.26 % and 2.6%.

In the experimental greenhouse, and with sonic 3D anemometers located near two screens and below one of the roof vents, values of the vertical component of the air velocity vector have been analysed for different scenarios of vent and screens opening percentages. We can conclude that if energy screens are used and with greenhouse natural ventilation openings usually open at low percentages, the measured values of the vertical resultant of air velocity vector near the screens are below 0.1 m s^{-1} for the majority of time, although at some specific periods they also can reach values between 0.1-0.2 m s^{-1}. Therefore, and for the purpose of characterizing the air permeability values of the different screens, a range of air velocities lower than 0.2 m s^{-1} should be suffice to characterize the screens aerodynamic properties properly. An air suction device measuring at low wind speeds is appropriate.

3.2.2 Measurement protocol Air suction device

A measurement protocol for the air suction device has to be established in order to reach maximum possible repeatability and to minimize measurement errors. Besides the intrinsic margins of error as a result from the accuracy of the pressure sensor, flow sensor and through polynomial regression (3.3.2 and Annex 2 Detailed description of model fitting procedure used to determine air permeability and resulting uncertainties), the overall system has been tested to validate its margin of error and identify additional error sources.
The following aspects have been tested:

- Repeatability.
- Effect of screen pattern size.
- Effect of relative orientation.
- To a very limited extent the homogeneity of screen materials.

Table 14

Repeatability measurements on two samples showing the measured permeability and the intrinsic uncertainty resulting from the device design

	LS16U sample 1		NT16M sample 1	
	Permeability	uncertainty	Permeability	uncertainty
Measurement 1	$8.54 \cdot 10^{-8}$	8 %	$2.76 \cdot 10^{-7}$	7 %
Measurement 2	$8.84 \cdot 10^{-8}$	7 %	$2.71 \cdot 10^{-7}$	7 %
Measurement 3	$8.49 \cdot 10^{-8}$	7 %	$2.74 \cdot 10^{-7}$	8 %
Measurement 4	$8.70 \cdot 10^{-8}$	8 %	$2.73 \cdot 10^{-7}$	8 %
Measurement 5	$8.61 \cdot 10^{-8}$	8 %	$2.73 \cdot 10^{-7}$	8 %
Measurement 6	$8.58 \cdot 10^{-8}$	8 %	$2.78 \cdot 10^{-7}$	6 %

Maximum variation is smaller than the uncertainty intrinsic in the measurement set-up, the standard deviation in the repeatability measurements is 1.3% for sample LS16U_sample1 and 0.8% for NT16M_sample1. So, the repeatability is better than the uncertainty.

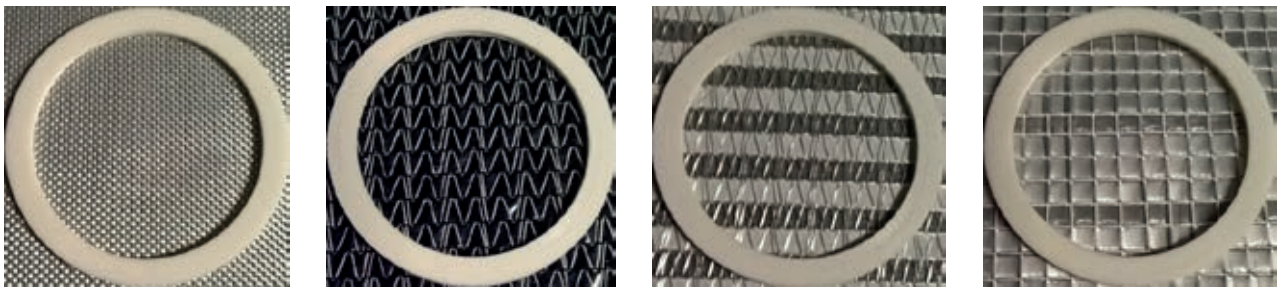

Figure 26 *Example of commonly encountered sample structure sizes.*

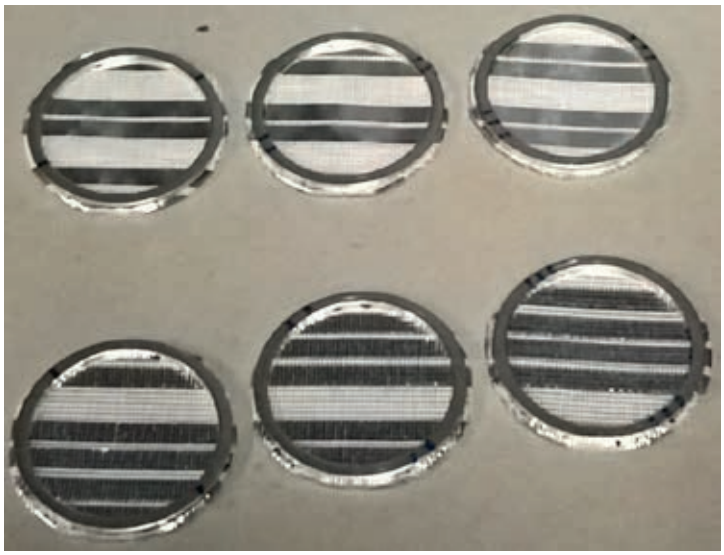

Figure 27 *Samples (NT16F) with large repeating structures sizes have been used to investigate the effect of structure size and replacement on measured permeability, above: NT16E, below: NT16F. For both screen materials, the aluminized part of the screen is completely closed (to every relevant degree) for air transport, while the white parts consist of an open structure.*

Table 15

Effects of screen pattern size of two materials showing the measured permeability and intrinsic uncertainties of the samples.

	NT16E (pattern size = 22 mm)		NT16F (pattern size = 36 mm)	
	Permeability	uncertainty	Permeability	uncertainty
Sample 1	$1.27 \cdot 10^{-6}$	7 %	$1.17 \cdot 10^{-6}$	6 %
Sample 2	$1.32 \cdot 10^{-6}$	10 %	$1.25 \cdot 10^{-6}$	6 %
Sample 3	$1.24 \cdot 10^{-6}$	8 %	$1.07 \cdot 10^{-6}$	6 %

The pattern size of sample NT16E (22 mm) seems to have influence on the obtained permeability, however, this variation is smaller than the uncertainty in the individual measurements. At a pattern size of 36 mm (NT16F) the variation caused by the different overlay of the sample pattern with the sample size is ~16% of the average permeability value, while the uncertainty within the measurements can only account for maximum ±6%.

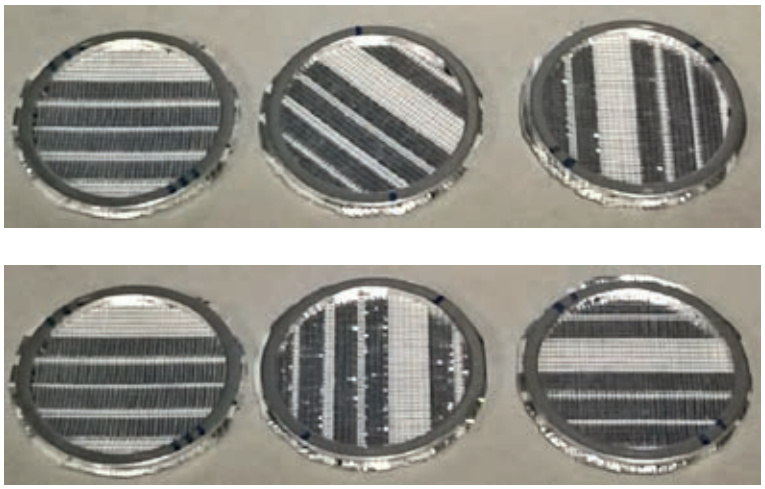

Figure 28 *The same samples which were used to investigate the effect of pattern size were also measured as a stack to investigate possible effects of relative orientation. The top row shows the orientation of subsequent samples measured in the '_twist45' configuration, the bottom row shows the '_twist90' configuration.*

Table 16

Effect of different relative orientation of a stack of three samples of two materials showing the measured permeability and intrinsic uncertainty of the samples.

	NT16E (sample 1, 2 and 3) (pattern size = 22 mm)		NT16F (sample 1, 2 and 3) (pattern size = 36 mm)	
	Permeability (of single sample)	uncertainty	Permeability (of single sample)	uncertainty
Parallel	$1.31 \cdot 10^{-6}$	5 %	$1.17 \cdot 10^{-6}$	7 %
Twisted 45°	$1.28 \cdot 10^{-6}$	6 %	$1.18 \cdot 10^{-6}$	5 %
Twisted 90°	$1.26 \cdot 10^{-6}$	6 %	$1.19 \cdot 10^{-6}$	6 %

The variation due to relative sample orientation is smaller than the uncertainty of the set-up.

On a very preliminary basis the degree of inhomogeneity in the two screen materials has been investigated, two materials were chosen which were judged to be homogeneous purely on visual inspection. 5 samples were prepared from each screen material in very close proximity to each other.

Table 17

Material homogeneity of five samples of two materials showing measured permeability and inherent device uncertainty of the samples.

	LS16U		NT16M	
	Permeability	uncertainty	Permeability	uncertainty
Sample 1	$8.54 \cdot 10^{-8}$	8 %	$2.76 \cdot 10^{-7}$	7 %
Sample 2	$8.89 \cdot 10^{-8}$	6 %	$2.51 \cdot 10^{-7}$	9 %
Sample 3	$8.51 \cdot 10^{-8}$	6 %	$2.59 \cdot 10^{-7}$	10 %
Sample 4	$9.14 \cdot 10^{-8}$	5 %	$3.20 \cdot 10^{-7}$	8 %
Sample 5	$7.85 \cdot 10^{-8}$	6 %	$3.03 \cdot 10^{-7}$	8 %

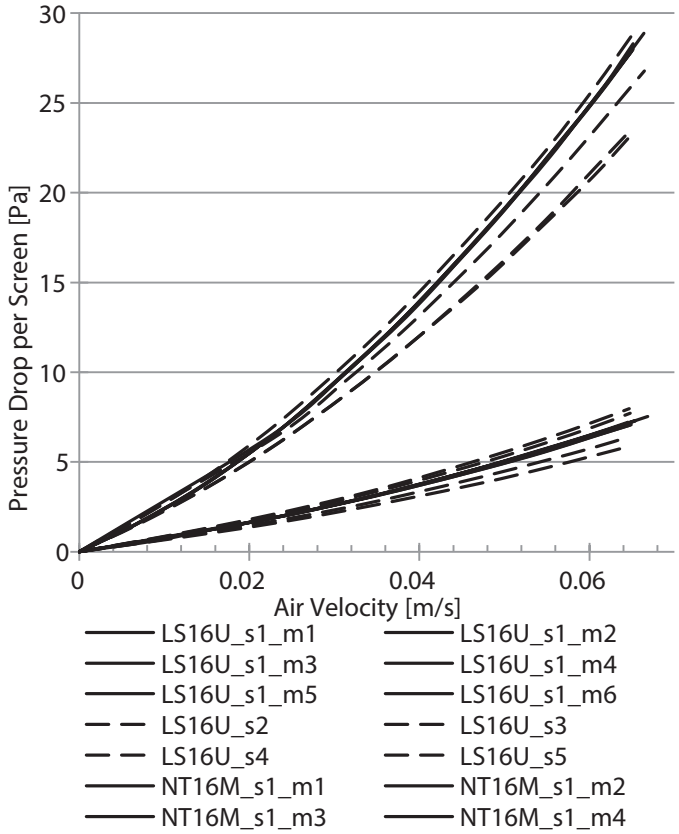

Figure 29 *Plotted air velocity and pressure difference measurements of two materials. The continuous lines are the repeatability measurements from which the permeability values in Table 14 were deduced. The dashed lines show the measurements investigating the homogeneity from which the permeability values in Table 17 were deduced.*

It has been shown that the device produced repeatable measurements within the margin of intrinsic uncertainty in the device. The variation observed investigating the effect of screen pattern size shows that probably a higher error has to be taken into account for pattern sizes larger than 2 cm. Even though this variation might also have been caused by inhomogeneity in the material, this limit was chosen to be on the save side.
The extent of inhomogeneity of materials has only very sparsely been investigated since this that was not within the scope of this project. As a result, the observed variation is very likely to be smaller than what to expect when sampling an entire screen instead of taking samples within a short distance from each other.

3.2.3 Measurement results screen materials

3.2.3.1 Wind tunnel measurements, high air velocity

Table 18 summarizes the aerodynamic characteristics of all 29 screens tested in the wind tunnel.

Table 18

Aerodynamic parameters of the 29 screens tested in the wind tunnel.

Code	χ (m)	K (m^2)	Y
CU16O	201	6.32E-10	0.1
CU16P	1503	1.60E-09	0.1
LS16U	329	2.20E-11	24.1
LS16V	301	1.93E-11	21.7
LS16W	286	1.73E-11	13.2
LS16X	273	2.68E-11	28.6
LS16Y	300	3.18E-11	50.5
LS16Z	372	3.30E-11	34.7
LS16Z1	412	2.14E-11	24.0
LS16Z2	276	1.36E-11	16.1
LS16Z3WB-BW	332	2.22E-11	15.6
LS16Z3WB+BW	303	3.19E-11	14.7
LS16Z4AB+B	369	2.31E-11	18.6
LS16Z4AB+B	286	9.44E-12	14.1
NT16C	636	---	---
NT16D	378	---	---
NT16E	346	2.16E-10	1.0
NT16F	372	4.21E-10	1.0
NT16G	261	5.82E-10	3.9
NT16H	447	1.83E-10	0.7
NT16I	248	2.37E-11	10.2
NT16J	366	2.16E-11	11.9
NT16K	260	2.48E-11	7.3
NT16L	301	1.89E-11	87.3
NT16M	153	1.28E-11	13.1
BP16A	62	---	---
BP16B	264	9,79E-12	16,17
BP16C	261	1,01E-11	20,05
BP16D	282	1,24E-11	30,36
BP16E	281	1,11E-11	41,31
BP16F-A	382	1,19E-11	14,08
BP16F-B	261	7,87E-13	7,88

---aerodynamic parameters of materials could not be measured due to low permeability

The most influential factor in the aerodynamic characteristics of a porous medium (here screen) is its porosity. Except the screens coded as CU16O, CU16P, NT16E, NT16F, NT16G and NT16H, the other tested screens are textiles with lower porosity; these textiles barely allow airflow through them. Furthermore, screens NT16C, NT16D and BP16A completely block the airflow, even for pressure differences greater than 800 Pa, for this reason it can be said that these screens are virtually impermeable to airflow to any meaningful extent in its current application. For screen BP16F-B it is possible to get a very small airflow (less than 0.15 m/s) when when applying a pressure difference of 1000 Pa.

Table 19 shows the results ranked by the ratio between the permeability K and screen thickness χ.

Table 19

Ratio between permeability K and screen thickness χ.

Code	χ (m)	K (m^2)	K/χ (m^2/m)
BP16F-B	261	7.87E-13	3.02E-09
BP16F-A	382	1.19E-11	3.12E-08
LS16Z4AB+B	286	9.44E-12	3.30E-08
BP16B	264	9.79E-12	3.71E-08
BP16C	261	1.01E-11	3.88E-08
BP16E	281	1.11E-11	3.94E-08
BP16D	282	1.24E-11	4.40E-08
LS16Z2	276	1.36E-11	4.95E-08
LS16Z1	412	2.14E-11	5.19E-08
NT16J	366	2.16E-11	5.90E-08
LS16W	286	1.73E-11	6.05E-08
LS16Z4AB+B	369	2.31E-11	6.26E-08
NT16L	301	1.89E-11	6.27E-08
LS16V	301	1.93E-11	6.43E-08
LS16Z3WB-BW	332	2.22E-11	6.69E-08
LS16U	329	2.20E-11	6.71E-08
NT16M	153	1.28E-11	8.40E-08
LS16Z	372	3.30E-11	8.87E-08
NT16K	260	2.48E-11	9.54E-08
NT16I	248	2.37E-11	9.57E-08
LS16X	273	2.68E-11	9.80E-08
LS16Z3WB+BW	303	3.19E-11	1.05E-07
LS16Y	300	3.18E-11	1.06E-07
NT16H	447	1.83E-10	4.10E-07
NT16E	346	2.16E-10	6.26E-07
CU16P	1503	1.60E-09	1.06E-06
NT16F	372	4.21E-10	1.13E-06
NT16G	261	5.82E-10	2.23E-06
CU16O	201	6.32E-10	3.14E-06

3.2.3.2 Air suction device measurements, low air velocity

Table 20 shows the results of the aerodynamic parameters of 7 selected screens measured with the air suction device at low air velocity. A comparison of permeability and margin of error is made with the permeability obtained in the wind tunnel at high air velocity.

Table 20

Comparison of aerodynamic parameters and errors of measurements on the air permeability device with low speed and in the wind tunnel with higher speed.

	Low speed air suction device at WUR		High speed wind tunnel in Almeria	
Sample	Permeability	Margin of error[1]	Permeability	Margin of error[2]
LS16U	$8.6 \cdot 10^{-8}$	8 %	$6.7 \cdot 10^{-8}$	61 %
BP16A	$1.9 \cdot 10^{-9}$	135 %	---	---
CU16O	$2.6 \cdot 10^{-6}$	10 %	$3.1 \cdot 10^{-6}$	18 %
NT16D	---	---	---	---
NT16E	$1.3 \cdot 10^{-6}$	6 %	$6.3 \cdot 10^{-7}$	26 %
NT16F	$1.2 \cdot 10^{-6}$	5 %	$1.1 \cdot 10^{-6}$	51 %
NT16M	$2.7 \cdot 10^{-7}$	8 %	$8.4 \cdot 10^{-8}$	34 %
NT16H	$5.2 \cdot 10^{-7}$	6 %	$4.1 \cdot 10^{-7}$	13 %
NT16K	$9.4 \cdot 10^{-8}$	5%	$9.5 \cdot 10^{-8}$	28 %

---aerodynamic parameters of materials could not be measured due to low permeability

[1] Margin of error is based on the combined error of the flow sensor, pressure sensor and regression analysis

[2] Margin of error is based on the error from regression analysis only

Permeability values are comparable within the margin of error. In general, the margin of error of measurements with the air suction device is lower. In both cases, impermeable materials or materials with low permeability cannot be measured.

3.3 Humidity transport through screens

3.3.1 Measurement results screen materials

3.3.1.1 Cup method measurements

Table 21 shows the results obtained in the measurements of humidity transport through each one of the 7 selected screen samples described in the methodology section, using the cup method protocol.

Table 21

*WVTR results according to ASTM E-96 norm at 19.4°C and 61% relative humidity expressed in g vapour per m^2 per day and per hour (n=3; *n=2).*

Sample code	WVTR ($g/m^2/d$) (19.4°C, 61-100% RH)	WVTR ($g/m^2/h$) (19.4°C, 61-100% RH)
LS-16-U	423 ± 5	17.6
BP-16-A	266 ± 9	11.1
CU-16-O	553 ± 37	23
NT-16-D	2.26 ± 0.85	0.09
NT-16-H	449.9 ± 19.3	18.7
NT-16-K*	449.9 ± 5.4	18.7
NT-16-M*	482.2 ± 6.5	20.1

The majority of the screens show rather similar values of humidity transport ranging from 18.7 $g/m^2/h$ and 23 $g/m^2/h$ for screens LS-16-U and CU-16-O, respectively. Only screens BP-16-A shows a rather small humidity transport, in agreement with the fact that this screen also showed a low value of air permeability. Screen NT-16-D was out of range in the permeability measurements and this low air permeability is also observed in the values of humidity transport, which are extremely low.

3.3.1.2 Swerea method measurements

Table 22 shows the humidity transport values measured using the Swerea method for seven selected screen samples. Figure 30 and Figure 31 also show a representation of the values, including the different repetitions of the measurement for each screen as well as the averaged value, respectively.

Table 22

Humidity transfer through screens.

	Humidity transfer ($g/m^2/h$)				
Screen:	No. 1	No. 2	No. 3	Average	Stddev
LS16U	50.3	42.8	47.5	47	3.8
BP16A	41.1	39.6	39.9	40	0.8
CU16O	138.5	143.7	150.9	144	6.2
NT16D	< 3	< 3	< 3	< 3	
NT16H	80.9	60.5	70.4	71	10.2
NT16K	48.4	47.0	50.3	49	1.6
NT16M	71.8	66.4	67.1	68	2.9

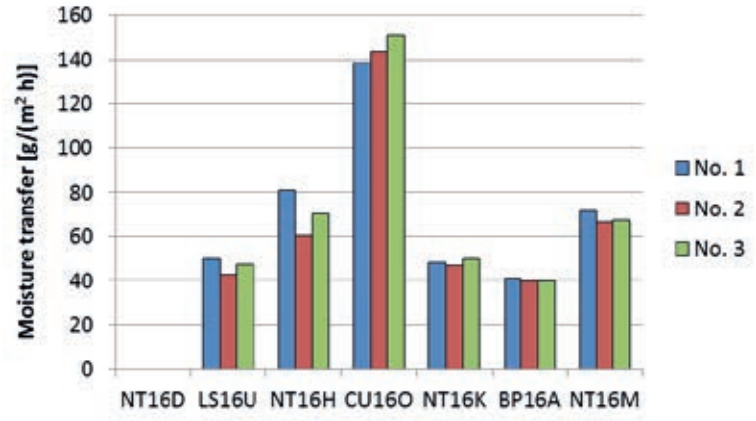

Figure 30 *Humidity transfer values measured for the 3 repetitions of each of the 7 screen sample.*

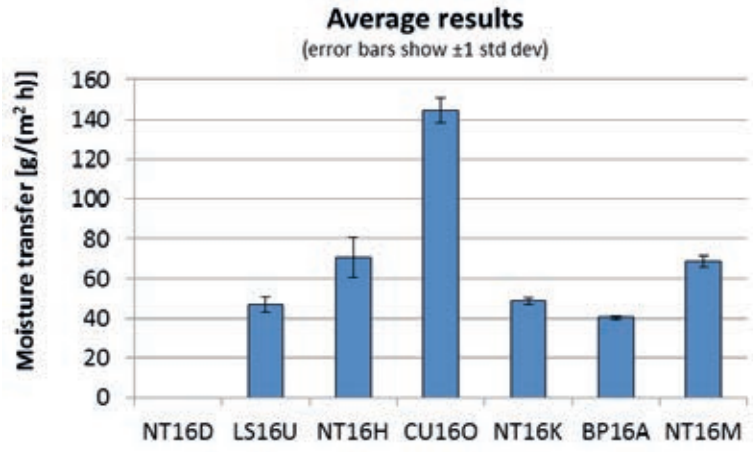

Figure 31 *Average humidity transfer values for each of the seven screen samples and standard deviation.*

Results indicate that the humidity transfer values measured under the conditions of the Swerea method are higher than those measured using the cup method. This proves that humidity transport is a combination of diffusion and other two mechanisms, that is convection and condensation/transport/re-evaporation. Figure 32 shows one of the screen samples just after finishing one of the experiments in Swerea. The image shows that condensation effectively occurs during the measurement, just as it is common in a greenhouse.

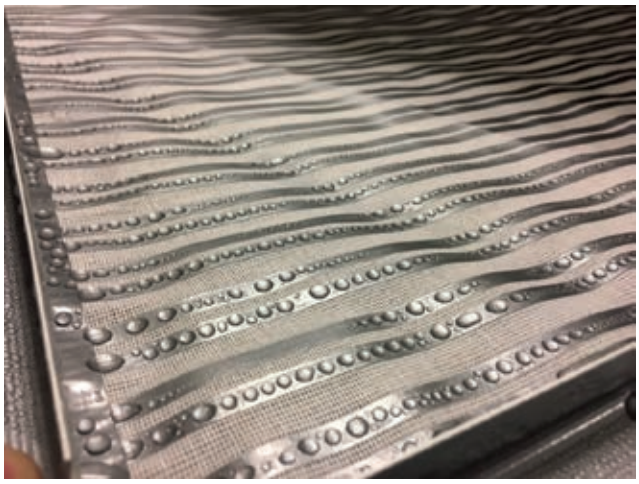

Figure 32 *Screen sample after experiments of Swerea.*

3.3.2 Modelling humidity transport by KASPRO

KASPRO simulations of the greenhouse microclimate with the usage of different combinations of screens have been widely validated with practical data concerning energy usage and realised climate parameters. However, detailed measured data of humidity transport through screens has not been used for validation. Therefore, humidity transport measurements performed for the Swerea method for seven different screens were used for a preliminary validation of the accuracy with which KASPRO calculates humidity transmission through the screen. For that, two different "special" weather data sets were generated in order to reproduce the same temperature and absolute humidity gradient conditions on both sides of the screens in KASPRO that were also used in Swerea experiments (Table 23).

Table 23
Testing conditions of Swerea method.

	Temperature gradient (°C)	Absolute humidity gradient (kg/kg)
Swerea method	10	0.0056

The simulations were run for a period of 3 days, and since the weather data file contained stable values for all the required parameters, this period of time was considered long enough to obtain reliable values.

Due to the dynamic nature of KASPRO, it was not possible to maintain completely stable conditions on both sides of the screen, which means that the temperature and absolute humidity gradient could not be maintained continuously at the same values but varied slightly around the set-point. However, for the majority of screens it was possible to maintain these values rather close to the experiments, so we can conclude that the values provided by KASPRO are representative enough for the experimental conditions.

Table 25 shows the values of humidity transport obtained from KASPRO and those obtained from the Swerea experiments.

Table 25
Comparison of humidity transport through different screens calculated by KASPRO and tested with Swerea method.

Sample code	Swerea ($g/m^2/h$)	KASPRO mean value ($g/m^2/h$)
LS-16-U	47	46.5
BP-16-A	11/40[2]	11.92
CU-16-O	144	80.7
NT-16-D	< 3	Not simulated[1]
NT-16-H	71	74.8
NT-16-K	49	47.88
NT-16-M	68	72.38

[1] This sample was not simulated as the value of air permeability of this screen could not be obtained nor in the wind tunnel experiments in Spain or in Wageningen with air suction device. The reason is that air permeability is so low that was out of the range of the measurement sensors.

[2] For screen BP-16-A two values are provided, corresponding respectively to the humidity transport value obtained during the first 10 hours of the experiment and to the rest of experiment when an increase in the slope of the humidity transport vs time curve was clearly observed.

The agreement for all screens in the KASPRO prediction of water humidity transport can be considered as very good, except for samples CU-16-O and for sample BP-16-A (if the second value of humidity transmission is considered, instead of the first one).

For sample CU-16-O the explanation for the low estimation of humidity transport performed by KASPRO may rely on the fact that for this screen, only a maximum temperature gradient of 2.2°C was obtained, far from the 10°C maintained in the experiments. This means that a larger temperature gradient would involve more buoyancy driven airflow through the screen and therefore a larger prediction of humidity transport by KASPRO. Next to the condensation and re-evaporation may be considered as dominant transport mechanism for this particular sample, which is in that case underestimated by KASPRO.
For sample BP-16-A, prediction is good when compared with the first value. If we accept that the dominant transport mechanism during the first 10 hours is convection, whereas from there on condensation and re-evaporation take a major role, we could conclude that KASPRO does a very accurate calculation of humidity transport by convection but underestimates the condensation-re-evaporation component. For the majority of the screens used for energy saving purposes, convection is surely the main humidity transport mechanism and therefore, KASPRO performs an accurate prediction, as we can see for all the other compared samples. However, for screens in which condensation/transport/re-evaporation is or can become after some time, the dominant transport mechanism, we can conclude that the humidity transport model that KASPRO uses at the moment may lead to an under-estimation of humidity transport values.

Results clearly indicate that the cup method is not the best methodology to estimate humidity transport through greenhouse energy saving screens, as it only measures the amount of humidity transported by diffusion, one of the three mechanisms of humidity transport, whereas the measurements performed in Swerea, which simulate better the conditions in the greenhouse, indicate that the other transport mechanisms also contribute largely to humidity transport (Table 25, Table 26).

Table 26

Humidity transport values(g/m^2. hour) measured using Swerea and cup method, respectively, for all the tested screen samples.

Sample code	Transport Swerea (g/m^2/h)/ Transport cup method (g/m^2/h)
LS-16-U	2.7
BP-16-A	3.6
CU-16-O	6.3
NT-16-D	not applicable
NT-16-H	3.8
NT-16-K	2.6
NT-16-M	3.4

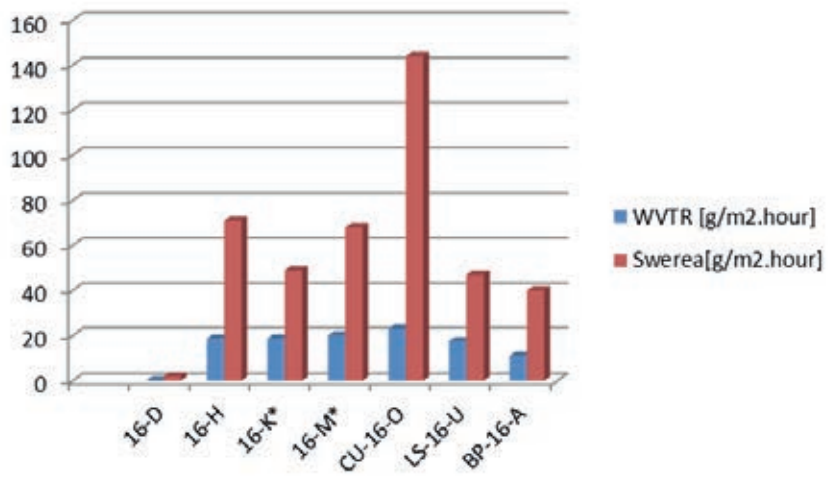

Figure 33 *Average humidity transport values measured at Swerea divided by average humidity transport measured with the cup method for each one of the tested samples.*

However, the Swerea methodology does not allow to distinguish how much of the transported humidity corresponds to each transport mechanism. Results with KASPRO simulations indicate that for the majority of tested screens the main transport mechanism seems to be convection through the screen. However, a detailed modelling of humidity transport through this type of screens is not yet available, thus, in order to know the humidity transport of a certain screen we still recommend to perform measurements using the Swerea methodology until a complete validated model is available.

3.4 Overall energy saving of screens

3.4.1 Modelling energy saving by KASPRO (dynamic model)

In a set of simulations, the different screens have been analysed. For the analysis of the energy saving of each screen, a year-round simulation has been run in which no screen was used for energy saving purposes in the greenhouse, in other year-round simulations each one of the different screens were used. Yearly energy usage and average energy saving for the whole year has been calculated. Next to that, the energy used only during the night hours (hours of screen usage) is calculated for the reference situation without screen and for each one of the different screens. Values of energy used during the hours that the screens are used during night hours are compared with this reference simulation.

Kaspro uses three main values measured in the lab for each one of the tested screens:
- Emissivity of the screen for thermal infrared radiation.
- Transmissivity of the screen for thermal infrared radiation.
- Air permeability of the screen.

Kaspro calculates the humidity transport by convection (based on air permeability) and condensation-transmission-re-evaporation.
In the day with the maximum energy saving if screens are used (10th January), both absolute amount of natural gas saved and in relative saving percentage are shown for each one of the different screens (Table 27, Figure 34).

Table 27

Total yearly energy used for heating (expressed as m^3 natural gas/m^2 greenhouse) for 7 different screens and the corresponding percentage of average energy saving (%), total yearly energy used for heating only during night hours and corresponding average energy saving during those night hours in relation to the reference, maximum daily energy saving in m^3/m^2 and %.

	Total yearly gas use (m^3/m^2)	Average energy saving[1] (%)	Total yearly gas use night hours (m^3/m^2)	Average energy saving night hours (%)	Maximum daily (24h) gas saving[2] (m^3/m^2)	Maximum energy saving during maximum gas saving night (%)
Reference, no screen	40.7	-	23.5	-	-	-
LS-16-U	33.9	16.7	16.5	29.7	0.086	32.9
BP-16-A	33.8	16.9	16.1	31.3	0.100	39.6
CU-16-O	37.2	8.6	20.4	13.2	0.037	16.5
NT-16-D	30.2	25.7	12.2	47.8	0.145	55.5
NT-16-H	34.9	14.3	17.8	23.9	0.063	28.5
NT-16-K	34.5	15.3	17.1	27	0.080	30.6
NT-16-M	34.5	15.3	17.3	26.1	0.071	31.9

1 Hours of use of screens: 2664

2 on January 10th

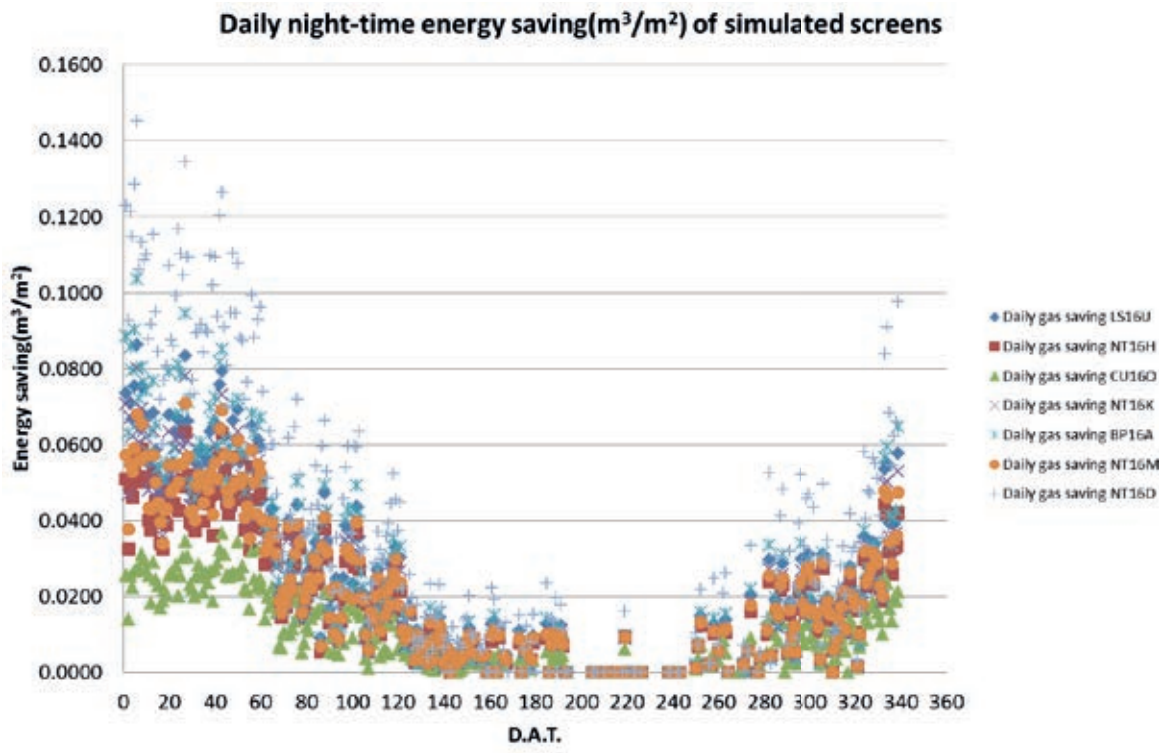

Figure 34 *Daily energy saved during the night time period (m^3/m^2) for 7 simulated screens during the growing cycle.*

Results indicate important differences between screens, screens with low air permeability NT-16-D and BP-16-A achieved a larger energy saving both in the whole cycle and during night hours and during the most energy consuming winter day. Energy saving of NT-16-D was 47.8% and of BP-16-A was 31.3% during night hours (maximum saving 55.5% and 39.6%, respectively). On the other side, for the most permeable screen CU-16-O the model provided lower values of energy saving (13.2%), also the maximum energy saving of CU-16-O was lower (16.5%).

Figure 35 and Figure 36 show the mean values and the mean of the maximum values of humidity transport through the screens (g/m^2/h), respectively, for the whole growing cycle. In these figures, we can see the difference in humidity transport through the different screens, with low values for the more impermeable screens (BP16A and NT16D) and high values for the very permeable screen (CU16O), which confirms that a higher latent heat loss is the reason for lower energy saving. The Figures also show that the highest values of humidity transport occur during the spring period, with a fully developed crop and the highest night time transpiration during the growing cycle.

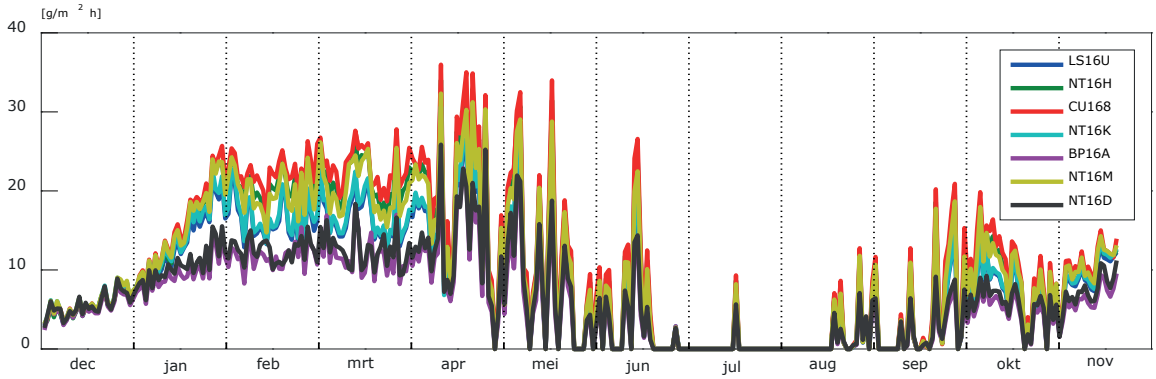

Figure 35 *Average humidity transport through each one of the simulated screens along the complete growing cycle during the night hours that screens are used.*

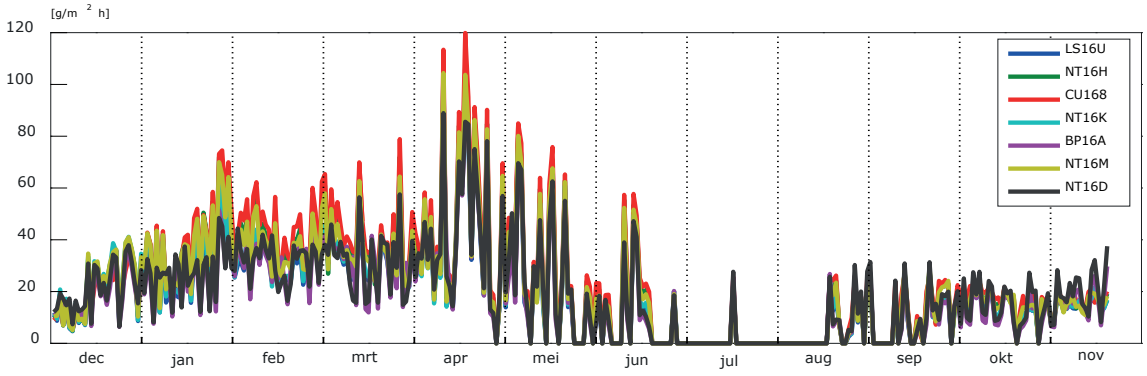

Figure 36 *Average maximum values of humidity transport through each one of the simulated screens along the complete growing cycle during the night hours that the screen is used.*

Calculations of total energy saving of screens with KASPRO are carried out in order to compare materials. We can state that identical air temperatures were realised under the screens according to the setpoint during the simulations (Figure 37), which is a requirement for fair materials comparison. The result is a difference in energy consumption based on materials properties, such as emissivity, air permeability and humidity transport.

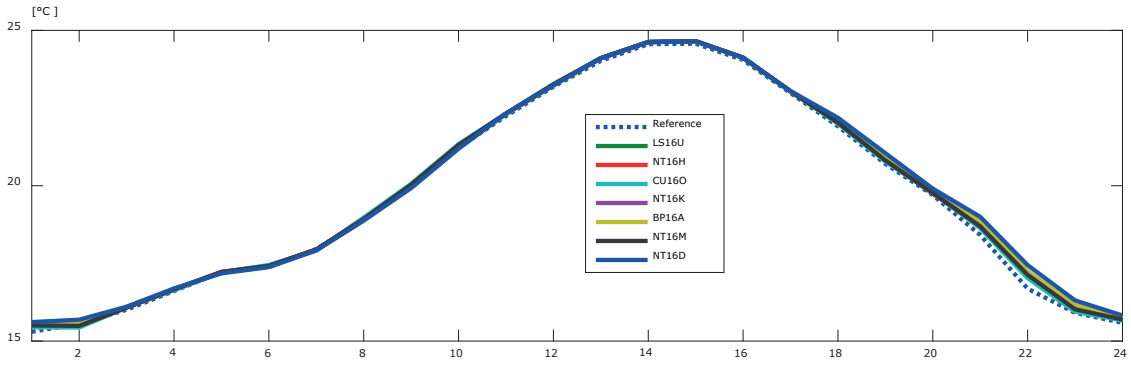

Figure 37 *24 hours cyclic mean of air temperature (°C) simulated by KASPRO for the reference scenario (no screen) and with the 7 screens samples tested and simulated, for the whole cycle.*

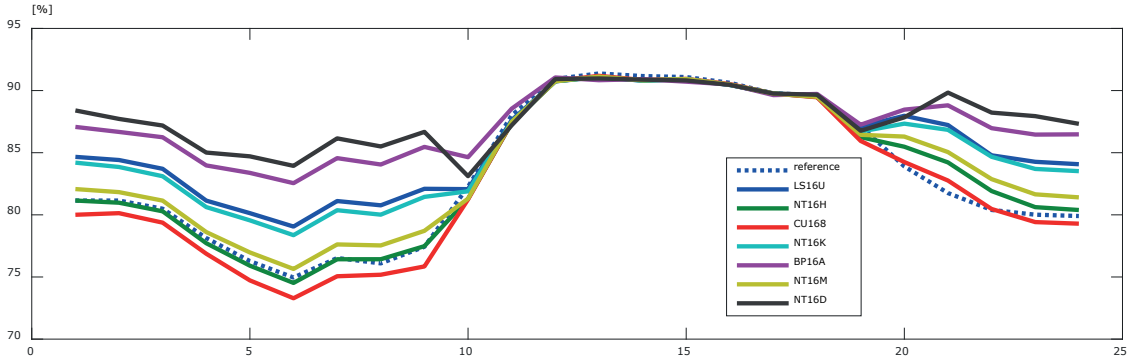

Figure 38 *24 hours cyclic mean of relative humidity (%) simulated by KASPRO for the reference scenario (no screen) and with the 67 screens samples tested and simulated, for the period between 15th October and end of the growing cycle.*

Figure 38 shows the cyclic mean of relative humidity values (%) for the reference case and under each one of the tested screens during the autumn, the most critical period for humidity due to full crop development (15th October-end of cycle). In the figure, we can also observe differences between screens. Highest humidity values are obtained below the impermeable screens NT16-D and BP16A screen due to low water vapour transport by convection, whereas lowest values of air humidity are obtained under CU16O screen due to highest values of water vapour transport.

In view of this graph, it might be surprising to see that relative humidity values are lower during the night time period than during the daytime. During this last part of the cycle, the LAI of the crop is decreasing and night-time transpiration values are quite low, whereas the screens can transport a large part of this transpired humidity, which then condensates on the greenhouse cover, as we can see in Figure 39 for screen LS16U.

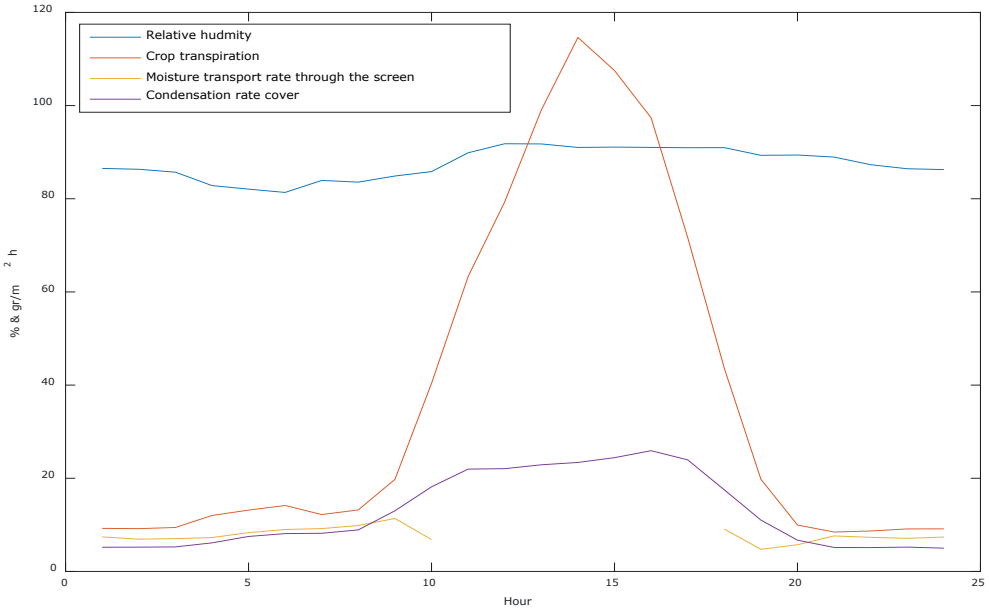

Figure 39 *24 hours cyclic mean of relative humidity (%), crop transpiration (g/m²/h), moisture transport rate trough the screen (g/m²/h) and condensation rate (g/m²/h) on the greenhouse cover for the period between 15th October and the end of the growing cycle, for screen LS16U.*

Values of relative humidity under CU16O predicted by the model are even lower during parts of the night than those under the reference greenhouse (no screen) (Figure 38). This indicates that the presence of the screen may induce a large proportion of water condensate in the roof thanks to the insulating effect of the screen. Figure 40 shows the simulation of total condensation for the reference greenhouse without screen and a greenhouse with CU16O screen. The presence of the screen allows for the roof to remain colder (less convection with internal heated air) and it allows enough humidity transport through the screen, which can then condensate in the roof, at higher rate than in the reference case during night hours. During daytime hours, negligible differences between the different scenarios can be observed.

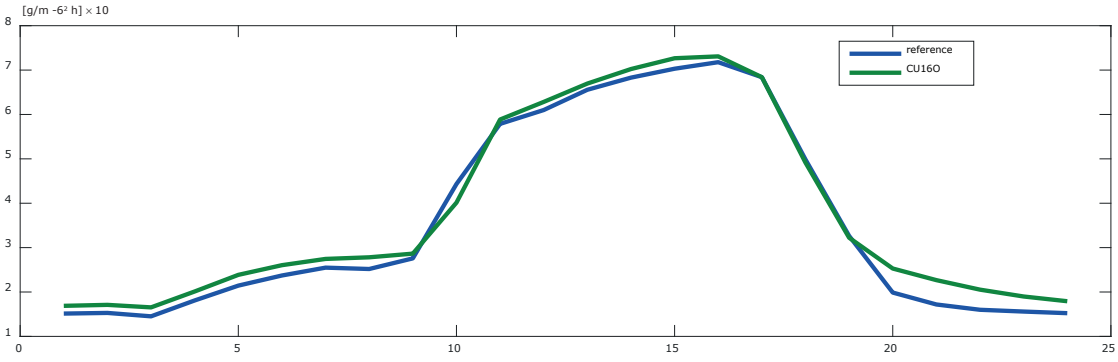

Figure 40 *24 hours cyclic mean of water condensation on the greenhouse cover (g/m²/h) simulated by KASPRO for the reference scenario (no screen) and with the CU16O screen sample for the period between 15th October and end of the growing cycle.*

Figure 41 shows, for one of the impermeable screens (BP16A) the mean of the values of water transport through the screens and crop transpiration (both in g/m^2/h) during the whole growing cycle on the nights that the screen is used. In this figure, we can see that during most of the cycle the average humidity transport values of this screen are smaller than the crop transpiration, thus the screen is not able to transport as much water per hour as the crop is producing. Thus, relative humidity under this screens will rise above the set point, showing the importance of using some kind of mechanical dehumidification systems if very impermeable screens are used. In general, energy consumption by mechanical dehumidification systems is much lower than additional energy saving of impermeable screens leading still to the highest energy saving of screens with low air and humidity permeability.

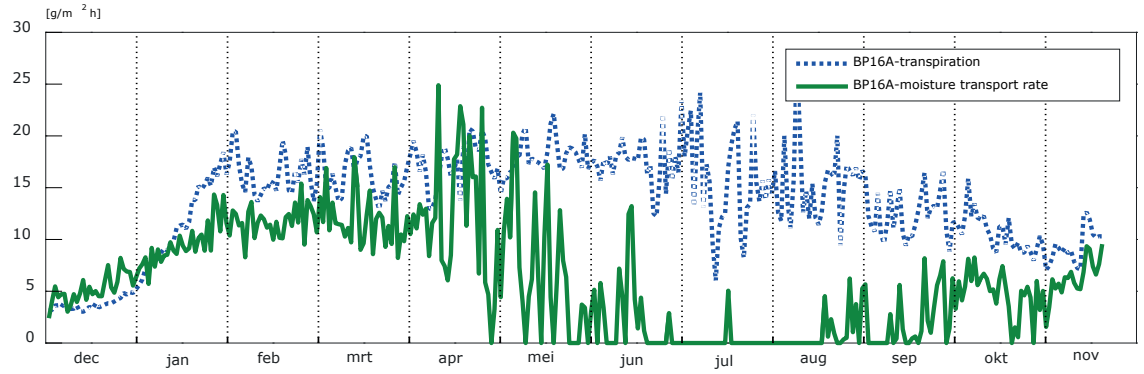

Figure 41 *24 h mean of maximum values of humidity transport and crop transpiration on nights where the screen is used for screen BP16A along the complete growing cycle.*

3.5 Summary of results

The total energy saving that can be realised by using screens in greenhouses is depending on its materials properties, such as emissivity, thermal infrared transmissivity and air and humidity permeability. These properties can be changed independently from each other but do all together influence the total (night time) energy saving. Because of that, also a set of screens with hypothetical properties has been simulated in which one property is kept the same while the other property is varied.

3.5.1 Effect of radiative properties

Hot heating pipes, warm crops and installations exchange heat radiation with the cold greenhouse roof and the cold sky. When the screens are closed, part of the thermal infrared (heat) radiation from inside the warm greenhouse is transmitted, reflected or absorbed and emitted by the screen material. That means that the radiative heat losses are reduced towards the cold roof and outside the greenhouse if any screen is used. If screens have a low absorption and emissivity for thermal radiation together with a low transmissivity for thermal radiation (all radiative heat reflected by the screen) this would lead to the highest possible energy saving for screens with the same air permeability.

Changing the thermal radiative properties of a screen, while keeping the air permeability fixed at 10^{-6} m^2 results in possible night time energy savings shown in Figure 42. Here the energy saving is shown in relation to the emissivity. Since a change in emissivity can coincide with an change in thermal infrared transmissivity (τ_{IR}) or a change in thermal infrared reflectivity (r_{IR}) (since $\varepsilon + \tau_{IR} + r_{IR} = 100\ \%$), the figure shows the effect on energy saving for screens depending on emissivity of screens with zero transmissivity or with zero reflectivity. It can be seen that for low emissivity a higher reflectivity r_{IR} increases energy saving while a larger transmissivity τ_{IR} decreases energy saving. This also means that a screen with this singular permeability can be anywhere in this triangular area depending on its radiative properties.

Conclusion: A screen with low emissivity and low transmissivity for thermal infrared radiation (and thus high reflectivity) leads to highest energy saving at the same air and humidity permeability.

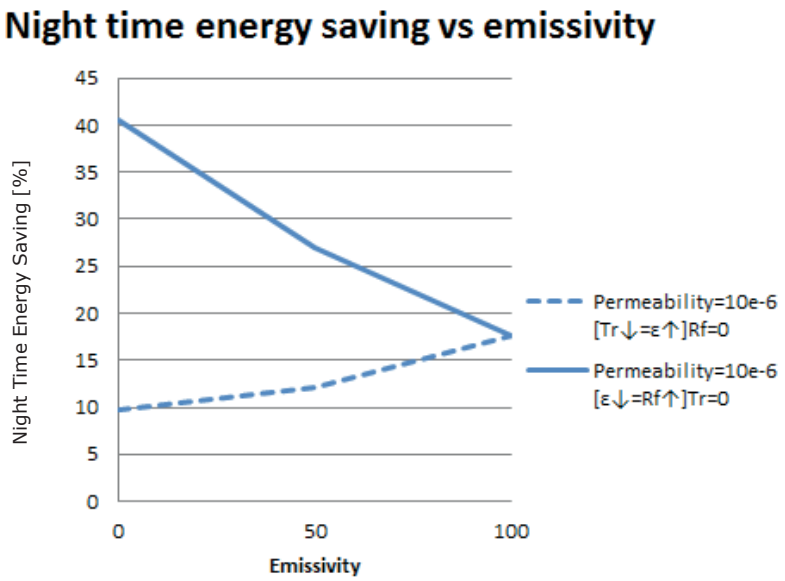

Figure 42 *Year-round night time energy saving as calculated by KASPRO simulations depending on the thermal radiative properties of a screen at a fixed air permeability. Dotted line: Screen with 0% thermal reflectivity with variable emissivity and transmissivity. Solid line: Screen with 0% thermal transmissivity and with variable emissivity and reflectivity.*

3.5.2 Effect of air permeability

For multiple permeability values Figure 43 is the extended version of Figure 42 where the night time energy saving is shown depending on emissivity for screens with both 0% transmissivity and 0% reflectivity for multiple air permeability values.

Conclusion: A screen with low air permeability leads to highest energy saving at the same thermal radiative properties. A combination of low air permeability with low emissivity and low transmissivity for thermal infrared radiation leads to highest energy saving.

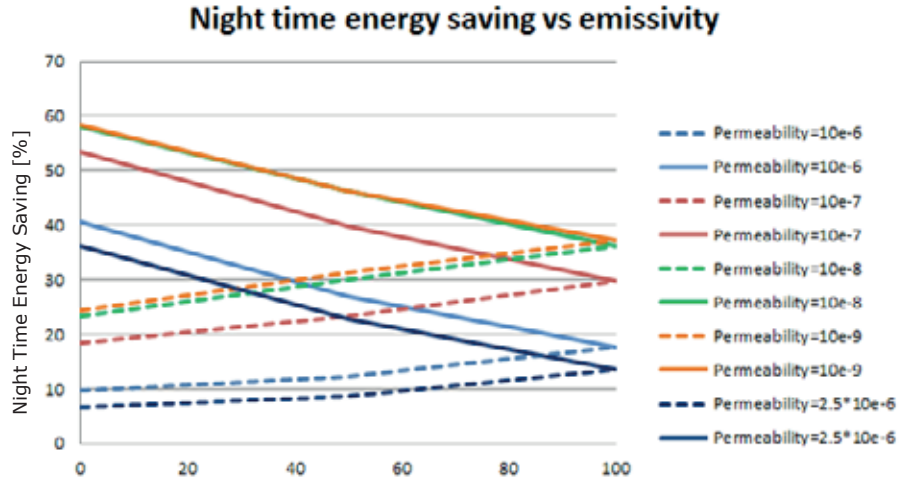

Figure 43 *Year-round night time energy saving as calculated by KASPRO simulations depending on the thermal radiative properties of a screen at different air permeability values. Dotted line: Screen with 0% thermal reflectivity and variable emissivity and transmissivity. Solid line: Screen with 0% thermal infrared transmissivity and variable emissivity and reflectivity.*

3.5.3 Effect of combined screen properties

Through buoyancy and convection processes warm and humid air is transported through a permeable screen, with that sensible and latent heat is removed from the crop area of the greenhouse and subsequently transported through the outer greenhouse cover. The result is an energy loss which is depending on the screen's air permeability where thermal radiative reflectance of 100% forms an upper bound and thermal radiative transmittance of 100% show a lower bound.

Figure 44 shows the relation of energy saving and radiative screen properties depending on the air permeability. The figure shows as well different combinations of theoretical screen properties (comparable with Figure 43) as measured screen properties of the 7 investigated screens.

Conclusion: A screen with low air permeability leads to highest energy saving especially combined with high thermal reflectivity (thus, low emissivity and low thermal transmissivity, green line). Only one of the screens comes close to that value, other screens show intermediate values for emissivity and thermal transmissivity.

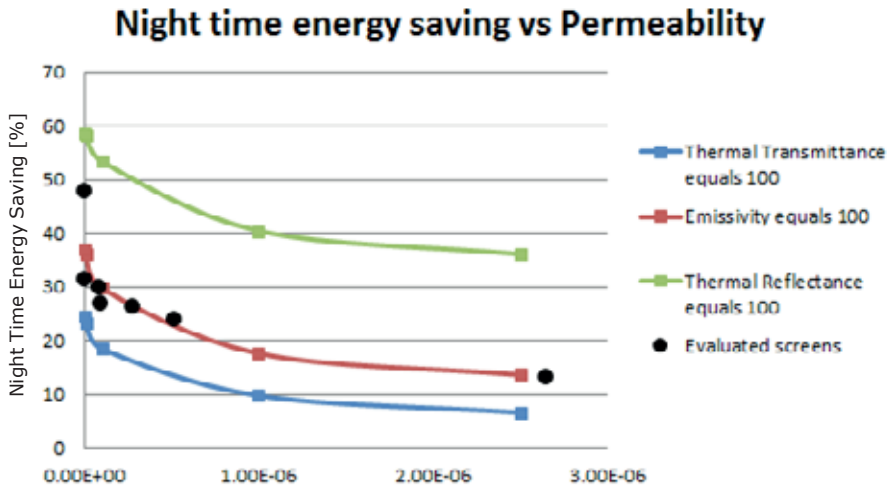

Figure 44 *Year-round night time energy saving as calculated by KASPRO simulations depending on the air permeability value of a screen. Different lines show different theoretical radiative screen properties, the blue line has 100% thermal infrared transmissivity and forms a lower limit for energy saving depending on permeability, the red line has 100% emissivity and the green line 100% thermal infrared reflectivity and represents an upper limit for energy saving depending on permeability). Black dots show measured screen properties of 7 screens.*

While the energy saving clearly increases with decreasing permeability, it must be noted that a low air permeability and low humidity transport values can lead to higher humidity levels in the greenhouse. Control of air humidity by mechanical dehumidification would be needed. Permeable screens give highest transport for humidity and lowest air humidity during screen usage without the need for additional mechanical dehumidification.

3.5.4 Effect of measurement uncertainty on total energy saving

The screen characteristics measured via the methods described in this report have some inherent uncertainty as has been described in previous sections of this report. For air permeability, it was shown that a relative uncertainty margin of ±8% is reasonable in most cases. For the thermal infrared properties, it was established that test-retest variability has a standard deviation of absolute 2-3% emissivity, transmissivity and reflectivity, to be 95% certain, a range of ±2 standard deviations, so ±5% absolute range of emissivity, transmissivity and reflectivity is reasonable.

To establish the uncertainty in the energy saving, the properties taking into account the least favourable and most favourable effect of the compound uncertainty is propagated into the KASPRO simulations and the resulting lower and upper results are taken as uncertainty margin in the energy saving. Of course, for the thermal properties the equation $\varepsilon + \tau_{IR} + r_{IR} = 100\,\%$ has to remain valid and since r_{IR} and τ_{IR} affect the energy saving in an opposing fashion they are adjusted in opposing directions, the emissivity is kept the same (Table 28).

Table 28

Lower and upper limit representing a 95% certainty range in the measured values which are propagated into the KASPRO simulations.

	Permeability*	r_{IR}*	τ_{IR}*	ε*
Lower limit energy saving	+8%	-5%	+5%	+0%
Higher limit energy saving	-8%	+5%	-5%	-0%

**Please note that the range for the permeability is relative to its absolute value, while the uncertainty range in the thermal properties is itself an absolute range of uncertainty.*

Table 29

Effect of the 95% confidence interval lower and upper limit on the night time energy saving for one screen (LS16U).

	Permeability	r_{IR}*	τ_{IR}*	ε*	Resulting night time Energy Saving
Lower limit energy saving	$9.32 \cdot 10^{-8}\,m^2$	15	38	47	27.9 %
LS16U	$8.63 \cdot 10^{-8}\,m^2$	20	33	47	29.8 %
Higher limit energy saving	$7.94 \cdot 10^{-8}\,m^2$	25	28	47	31.8 %

While it may seem counter intuitive that a variation of 10% in the thermal properties of a screen results in only 4% variation in night time energy saving, this can be easily explained by the fact that the thermal radiative properties affect only a range of 30~35% of absolute energy saving and the relative uncertainty in permeability is small relative to the 4 orders of magnitude range of permeability values we encountered in this project.

Conclusion: The uncertainty of different measurements of screen properties determined (chapter 3.1 and 3.2) lead to +/-2% variation in total energy saving of a screen material.

4 Recommendations

In this study, different methods and procedures for determining single screen material properties have been evaluated and developed. We recommend screen producers to obtain the following material properties for their materials and provide this information to growers. Growers can use this information to make a choice for a screen material depending on crop and requirements.

- Emissivity, thermal infrared transmissivity and reflectivity of screens.
- Air permeability of screens.
- Humidity transport of screens.
- Calculation of total energy saving key figures.

Emissivity ε should be reported next to thermal infrared transmissivity τ_{IR} and reflectivity r_{IR}, all in %. TNO emissivity meter can be used as equipment. A procedure is given in this report.
Air permeability should be reported in terms of permeability K, in m^2. A figure of permeability depending on air velocity should be given. An air suction device can be used to determine air permeability of screens for low air velocities. A description of the equipment is given in this report. A measurement procedure is given in this report.
Humidity transport of screens should be measured following the Swerea method. The cup method is not suitable. A description of the experimental set-up and measurement procedure is given in this report. Results should be reported in water vapour transport in $g/m^2/h$.
Total energy saving of screens should be calculated with KASPRO. The assumptions given in this report should be used for calculations. The same key figures for total yearly energy consumption, total yearly energy saving, energy saving during night hours and maximum saving should be reported. Next to that a figure of expected daily humidity transport through the screen should be reported.

Screen producers should decide if they want to have all different measurement equipment for determining single screen material properties available at their own company.
Screen producers should decide if they need a central independent research lab to be able to carry out all different measurements. Both, TNO emissivity and air suction device are available at WUR for independent measurements of screen materials. In the future modifications of equipment could lead to further improvement of accuracy of measured values. Currently the measurement of humidity transport through screens is not available in The Netherlands. In case such equipment should be made available for the Dutch greenhouse sector, equipment could be developed in a follow-up project.
Screen producers should decide if they want to have a simple calculation programme in order to calculate total energy saving of a screen material available at their own company. Calculations of total energy saving of screens can currently be carried out at WUR. A simple program with fixed assumptions and fixed output could be made available in a follow-up project.

Growers can select a specific screen material based on single screen material properties and total energy saving potential. Impermeable screens and screens with low emissivity and low thermal infrared transmissivity and emissivity give highest energy saving. However, additional mechanical dehumidification might be needed depending on the crop requirements. Permeable screens give highest transport for humidity and lowest air humidity during screen usage without the need for additional mechanical dehumidification.

Literature

De la Faille, B. J.B. Campen, H. Oversloot (2009).
Emission and transmission of heat radiation through screens. TNO rapport 034-DTM-2009-04659

De Zwart, H.F., 1996.
Analysing energy saving options in greenhouse cultivation using a simulation model, PhD thesis, Wageningen University, p. 236.

Goudriaan, J.; H.H. Van Laar. 1994.
Modelling Potential Crop Growth Processes. Textbook with Exercises, Kluwer Academic Publishers, Dordrecht (1994) 238 pp.

Molina-Aiz, F.D.; Valera, D.L.; Peña, A.A.; Gil, J.A.; López, A. 2009.
A study of natural ventilation in an Almería-type greenhouse with insect screens by means of tri-sonic anemometry. Biosystems Engineering 104: 224–242.

Miguel A.F.; Van de Braak N.J.; Bot G.P.A. 1997.
Analysis of the airflow characteristics of greenhouse screening materials. J Agr Eng Res 67, 105-112.

Miguel A.F. 1998.
Transport phenomena through porous screens and openings: from theory to greenhouse practice. Doctoral Thesis. Agricultural University of Wageningen, Holland. 239 pp

Wang, S.; M. Yernaux, J.; Deltour, A. 1999.
Networked Two-Dimensional Sonic Anemometer System for the Measurement of Air Velocity in Greenhouses, Journal of Agricultural Engineering Research, Volume 73, Issue 2, 1999, Pages 189-197, ISSN 0021-8634, http://dx.doi.org/10.1006/jaer.1998.0403.

5 Aanleiding en Projectdoel

Schermen worden in de praktijk in diverse uitvoering (weefsels, breisels of folies, open of dichte structuren, transparant, diffuus, gealuminiseerd of diverse kleuren) en voor diverse doelen (energiebesparing, vermindering lichtsom, diffuus licht of verduistering) gebruikt. Een belangrijk doel van schermen in Nederlandse kassen is energiebesparing. Helaas is er tot op heden geen objectieve methode om de energiebesparing van een doek onder vergelijkbare omstandigheden vast te stellen. Energiebesparingspercentages worden door leveranciers volgens verschillende methodes ingeschat. Tuinders hebben zo weinig mogelijkheden om schermprestaties onafhankelijk met elkaar te kunnen vergelijken om tot een afgewogen investeringsbeslissing te komen.
Dit probleem is al langer bekend. Een eerste stap om dit op te lossen is eerder gemaakt in het project "Emissiewaardes van schermen", uitgevoerd door TNO, WUR en 2 schermfabrikanten. Dit heeft geleid tot een objectieve meetmethode en apparaat voor het bepalen van de emissiewaarde van schermen. Dit is echter niet voldoende om de energiebesparing van schermen te bepalen. Deze wordt namelijk niet alleen bepaald door de stralingsdoorgang (transmissie en emissie van warmtestraling) maar ook door de luchtdoorgang (convectie bij lage windsnelheiden) en door de vochtdoorgang (lucht- en daarmee vochtdoorgang en vochttransport in bandjes, garens, plastics door diffusie, absorptie of adsorptie). Het is nodig om alle genoemde schermeigenschappen onder geconditioneerde omstandigheden te meten en daarna met een fysisch model de energieprestaties voor schermen voor een gedefinieerde situatie te berekenen. Op deze manier kunnen materialen met elkaar worden vergeleken. Het ontwikkelen van de juiste meetmethodes, protocollen en berekeningsmethodieken voor deze materiaalvergelijking is het doel van het hier beschreven project.
De uiteindelijke energiebesparing in de praktijk hangt echter ook af van de scherminstallatie en het gebruik door de tuinder (schermmoment, aantal schermuren) en zal hier niet worden behandeld. In de toekomst is het zinvol om ook vergelijkende metingen van verschillende materialen met bekende eigenschappen in een kas te doen.

De doelstellingen van dit project waren, het kwantificeren van de schermeigenschappen (emissie, transmissie, lucht- en vochtdoorgang) en het bepalen van de energiebesparing onder gedefinieerde omstandigheden om de energieprestaties van verschillende schermen (en leveranciers) met elkaar te kunnen vergelijken. Dit geeft de tuinders inzicht en maakt een bewuste keuze mogelijk. Dit zal de inzet van goed isolerende schermen in de toekomst, ook in het kader van HNT, verder bevorderen.
Wanneer de energiebesparing van verschillende schermen (en leveranciers) eenduidige kunnen worden vastgesteld, geeft dit informatie voor fabrikanten om nog betere producten te ontwikkelen en geeft dit informatie voor tuinders om bewust een schermtype te kiezen. Het geeft inzicht in luchtdoorgang en vochtdoorgang van schermen naast de totale energiebesparing. Door een bewustere omgang van tuinders met schermen kan naar verwachting 5% meer energie worden bespaard. Daarnaast was het doel het beschikbaar stellen van objectieve meetmethodes, -protocollen en berekeningsmethodieken aan de sector en toeleverende industrie.

6 Resultaten en Samenvatting

Schermen worden in de praktijk in diverse uitvoering (weefsels, breisels of folies, open of dichte structuren, transparant, diffuus, gealuminiseerd of diverse kleuren) en voor diverse doelen (energiebesparing, vermindering lichtsom, diffuus licht of verduistering) gebruikt. Een belangrijk doel van schermen in Nederlandse kassen is energiebesparing. Helaas is er tot nu toe geen objectieve meet- of rekenmethode om de energiebesparing van een schermmateriaal te bepalen onder gedefinieerde omstandigheden.

In dit onderzoek zijn verschillende methoden en procedures voor het bepalen van de materiaaleigenschappen van schermen geëvalueerd en ontwikkeld. De totale energiebesparing van een scherm materiaal wordt bepaald door de stralingsuitwisseling (transmissie en emissie voor warmtestraling), de luchtdoorlaat door het scherm (convectie bij lage windsnelheden) en het transport van vocht door het materiaal (lucht en daarmee transport van vocht en transport van vocht door garens of kunststoffen door diffusie, absorptie of adsorptie). Het is noodzakelijk om al deze scherm eigenschappen onder gecontroleerde omstandigheden te meten en dan gebruik te maken van een rekenmodel om de energieprestatie van schermen voor een vooraf vastgelegde situatie te berekenen. Zo kunnen materialen met elkaar worden vergeleken.

Het doel van het project is de **ontwikkeling van geschikte meetmethoden, protocollen en een berekeningsmethode om schermmaterialen met elkaar te kunnen vergelijken**. Verder zijn de doelstellingen van het project het kwantificeren van diverse scherm eigenschappen (emissie, luchtdoorlatendheid en vochttransport) en de berekening van de totale energiebesparing onder bepaalde omstandigheden voor verschillende geselecteerde schermmaterialen.

De **emissie** van geselecteerde scherm monsters is gemeten op de eerdere door TNO ontwikkelde Emissie meter (De la Faille *et al.,* 2009). Emissie waardes verschillen grotendeels tussen de verschillende schermmaterialen. Terwijl onderzochte materialen BP16A en NT16D zeer lage emissie waardes (<10%) hadden, toonden andere materialen zoals NT16K, LS16U en CU16O gemiddelde of hoge waarden (NT16H en NT16M,> 60%). Emissie waarden kunnen verschillende aan beide kanten van een schermmateriaal afhankelijk van de samenstelling. Daarnaast laten materialen NT16M, NT16H en ook NT16D en CU16O een lage transmissie voor warmtestraling zien (<30%). Echter, alleen materiaal NT16D heeft een combinatie van lage emissie en lage transmissie voor warmtestraling, met gelijktijdig een hoge reflectie. De combinatie van lage emissie en lage transmissie (hoge reflectie) leidt in het algemeen tot een hoge energiebesparing.

De **luchtdoorlatendheid** van scherm monsters is gemeten, zowel bij lage windsnelheden met de WUR Permeabiliteitsmeter en bij hoge windsnelheden in een windtunnel aan de Universiteit van Almeria. De luchtdoorlatendheid is grotendeels afhankelijk van de samenstelling van de schermmaterialen. Terwijl materialen CU16O (glasvezel non-woven), NT16E (poreus met 4 aluminium bandjes) en NT16F (poreus met 2 aluminium bandjes) een extreem hoge luchtdoorlatendheid hebben, tonen LS16U (gebreid met transparante bandjes), NT16M (glasvezel geweven), NT16H een gemiddelde permeabiliteit, anderen zoals NT176D (gelamineerd met transparante en aluminium strips) en BP16A (transparant geweven) hebben een extreem lage luchtdoorlatendheid en daarmee een kleiner verlies van voelbare en latente warmte. In het algemeen leidt een lage luchtdoorlatendheid tot een hogere energiebesparing.
In een commerciële kas zijn metingen van de luchtsnelheid met 3D-anemometers uitgevoerd voor verschillende scenario's van ventilatie- en schermpercentages. We kunnen concluderen dat indien energieschermen gebruikt worden en natuurlijke ventilatieopeningen met een kleine percentage geopend zijn, de gemeten luchtsnelheden dicht bij de schermen voor het merendeel van de tijd kleiner dan 0,1 m/s zijn, alleen in een aantal specifieke periodes worden waardes tussen 0,1-0,2 m/s bereikt. Indien voor metingen van de luchtdoorlatendheid van materialen luchtsnelheden lager dan 0,2 m/s worden gebruikt, kunnen de aerodynamische eigenschappen van schermen goed worden gekarakteriseerd. Metingen met de WUR Permeabilitietsmeter bij lage windsnelheden zijn hiervoor geschikt. Windtunnel metingen bij hoge luchtsnelheden zijn niet nodig om schermprestaties te karakteriseren.

Het **vochttransport** scherm monsters is gemeten door twee verschillende meetprincipes. In de cup methode wordt een absoluut vochtgradiënt aan twee kanten van het scherm monster aangehouden, water moet diffunderen door het monster langs de vochtgradiënt. In de cup methode wordt de waterdamp transmissiesnelheid (WVTR), gemeten volgens ASTM E96.
Een beperking van de cup methode is dat zij slechts rekening houdt met één van de vochttransport mechanismes door een poreus materiaal (hier een scherm), namelijk diffusie. In een praktijk kas worden echter energieschermen geplaatst zodat deze twee kascompartimenten van elkaar scheiden, één onder het scherm, waar verwarmingssysteem en gewasverdamping een warme en vochtige lucht creëren, en één boven het scherm, waar de lucht kouder en droger is. Zo ontstaat er naast een vochtgradiënt ook een temperatuurgradiënt. Dit betekent dat er afhankelijk van de luchtdoorlatendheid van het scherm een luchtstroom door het materiaal ontstaat gedreven door natuurlijke of geforceerde convectie (afhankelijk van de opening van de natuurlijke ventilatie of de aanwezigheid van ventilatoren). Deze convectieve luchtstroom voert ook waterdamp mee, die door de cup methode niet gekwantificeerd kan worden. Bovendien zal de temperatuurgradiënt aan beide zijden van het scherm ook leiden tot condensatie aan de binnenkant van het scherm wanneer de schermtemperatuur lager dan het dauwpunt wordt. Mocht dit gebeuren, wordt een deel van het gecondenseerde water door het scherm getransporteerd en aan de andere kant weer verdampt. Ook dit extra mechanisme wordt niet gekwantificeerd door de cup methode. Nieuwe meetapparatuur en protocollen moeten worden gebruikt welke op een realistische manier de kas omstandigheden simuleren en welke het totale transport van vocht door een scherm kunnen kwantificeren. Swerea instituut, Zweden, heeft een dergelijke specifieke methode (Swerea IVF 82-11) ontwikkeld om metingen van de waterdamp transmissiesnelheid door schermen uit te voeren in een klimaatkamer.
Resultaten geven aan dat de vochtdoorlatendheid van schermen gemeten onder de omstandigheden van Swerea hoger zijn dan die gemeten door de cup methode. Dit bewijst dat transport van vocht een combinatie is van diffusie en twee andere transport mechanismes, convectie en condensatie / transport / verdamping. Gemeten scherm materialen NT16D en BP16A tonen een laag vochttransport, anderen zoals SL16U, NT16H en NT16M laten gemiddelde waardes zien, voor CU16O wordt het hoogste vochttransport gemeten. In het algemeen zorgt een laag vochttransport voor een hogere energiebesparing. Het kan echter noodzakelijk zijn om een extra mechanisch ontvochtigingssysteem in de kas te gebruiken om aan de eisen van het gewas te voldoen.

De **totale energiebesparing** van schermen is sterk gerelateerd aan de materiaaleigenschappen, zoals emissie, luchtdoorlatendheid en vochttransport. Het model KASPRO (de Zwart, 1996) wordt gebruikt voor de berekening van de totale energiebesparing onder vooraf bepaalde omstandigheden.
In het algemeen bespaart het gebruik van een energiescherm energie ten opzichte van een kas zonder scherm. De resultaten van de berekende energiebesparing van de geselecteerde schermen laten een duidelijk verband tussen de luchtdoorlatendheid waardes van elk scherm en de energiebesparing zien. Door buoyancy, diffusie en convectie processen wordt warme en vochtige lucht door een luchtdoorlatend scherm getransporteerd, voelbare en latente warmte wordt hiermee uit de kas verwijderd. Het resultaat is een energieverlies afhankelijk van de hoeveelheid luchtdoorlatendheid van het materiaal.
De resultaten van de berekende energiebesparing van de geselecteerde schermen laten ook een duidelijke relatie tussen de emissie waarde van elk scherm en de energiebesparing zien. Hete verwarmingsbuizen, warme gewassen en installaties wisselen warmtestraling uit met het koude kasdek en de koude lucht. Wanneer de schermen worden gesloten, wordt een deel van deze warmte straling vanuit de warme kas door het schermmateriaal geabsorbeerd en aan de bovenkant weer geëmitteerd. Dat betekent dat stralingswarmte verloren gaat naar het koude dak en buiten de kas. Het energieverlies is afhankelijk van de emissie waarde van het scherm.

Schermmateriaal NT16D toont de hoogste totale energiebesparing met een jaarlijkse besparing van gemiddeld ca. 25% (op basis van het energieverbruik van alle uren, slechts 2664 uur waren schermuren) of ca. 48% op basis van alleen de uren waarin de schermen worden gebruikt. Dit scherm heeft een lage luchtdoorlatendheid, een lage emissie en een lage transmissie voor warmtestraling. Materialen BP16A, LS16U, NT16H, NT16K en NT16M tonen jaarlijks een gemiddelde besparing van ca. 14-17% over alle uren of ca. 25-30% uitsluitend gebaseerd op de uren waarin de schermen worden gebruikt. De laagste energiebesparing werd berekend voor CU16O, dit scherm heeft wel het hoogste vochttransport. Schermen BP16A en NT16D hebben de hoogste maximale energiebesparing tijdens de koudste nacht. Beide schermen hebben het laagste vochttransport wat tot een hoge besparing leidt. Echter, tijdens piekuren van de gewasverdamping is het vochttransport door de schermen kleiner dan de verdamping. Dit maakt het belang van het gebruik van een soort mechanisch ontvochtigingssysteem duidelijk, indien zeer dichte, niet-doorlatende schermen worden gebruikt. In het algemeen is het extra energieverbruik van mechanische ontvochtigingssystemen veel lager dan de extra energiebesparing door dichte schermen en leiden schermen met een lage lucht- en vocht doorlatendheid nog steeds tot de hoogste energiebesparing.

Uit de resultaten van het project adviseren wij **scherm producenten** om de volgende materiaaleigenschappen voor hun materiaal te kwantificeren en deze informatie aan telers door te geven. Telers kunnen deze informatie gebruiken om een keuze te maken voor een bepaald schermmateriaal afhankelijk van de eisen van hun teelt.

- Emissie waarde schermen.
- Luchtdoorlatendheid schermen.
- Vochttransport van schermen.
- Berekening van kengetallen van de totale energiebesparing.

De emissie warde ε moet naast de transmissie van warmtestraling τ_{IR} en de reflectie van warmtestraling r_{IR}, allemaal in %, worden vermeld. De TNO Emissie meter kan voor deze metingen worden gebruikt. Een meetprocedure wordt beschreven in dit rapport.
De luchtdoorlatendheid dient te worden gerapporteerd in termen van permeabiliteit K, in m^2. Een figuur van de permeabiliteit afhankelijk van de luchtsnelheid moet worden weergegeven. De WUR Permeabiliteitsmeter kan worden gebruikt om luchtdoorlatendheid van schermen voor lage luchtsnelheden te meten. Een beschrijving van de apparatuur wordt gegeven in dit rapport. Een meetprocedure wordt beschreven in dit rapport.
Het vochttransport door schermen moet worden gemeten volgens de Swerea of een vergelijkbare methode. De genormeerde cup methode is niet geschikt. Een beschrijving van de experimentele setup en meetprocedure wordt gegeven in dit rapport. De resultaten van de vochtdoorlatendheid moeten worden vermeld in waterdamp transmissiesnelheid, in $g/m^2/h$.
De totale energiebesparing van schermen moeten worden berekend met een model zoals KASPRO. De aannames die in dit rapport beschreven worden moet worden gebruikt voor berekeningen. Dezelfde kengetallen voor het totale jaarlijkse energieverbruik, de totale jaarlijkse energiebesparing, de energiebesparing tijdens schermuren en de maximale besparing moeten worden vermeld. Daarnaast moet een figuur van het verwachte dagelijkse vocht transport door het scherm worden weergegeven.

Telers kunnen een specifiek scherm selecteren op basis van één of meerdere specifieke materiaaleigenschappen of op basis van de potentiele totale energiebesparing van het materiaal. Dichte, niet-luchtdoorlatende schermen en schermen met lage emissie waardes en lage transmissie van warmtestraling geven de hoogste energiebesparing. Het is echter mogelijk dat een extra mechanisch ontvochtigingssysteem nodig is, afhankelijk van de behoeften van een gewas. Doorlaatbare schermen geven het hoogste vochttransport en de laagste luchtvochtigheid tijdens scherm gebruik zonder de noodzaak voor een extra mechanisch ontvochtigingssysteem.

Annex 1 Overview of samples

Low & Bonar
Six different samples are delivered by Low & Bonar. The WUR codes and descriptions of producer is as follows:

- BP16A: Phormitex Clear consists of woven transparent bands with no threads.
- BP16B: Phormitex Bright is woven from transparent bands with threads.
- BP16C: Clima 45+ is constructed from woven white & transparent bands. The repeating pattern is as follows: 2xTr + 1xW + 1xTr + 1xW.
- BP16D: Clima 65+ is also constructed from woven white & transparent bands. The repeating pattern is as follows: 4xW + 1xTr.
- BP16E: PH77 is constructed from aluminized & diffuse bands. The repeating patteren is: 3xAl + 1xDiffuse.
- BP16F: Eclipse 98 which is fully aluminized on one side and the bottom side is fully black + Eclipse 1 which is a completely black screen.

An overview of Low & Bonar screens is presented in Figure 45.

Phormitex Clear /BP16A.

Phormitex Bright /BP16B.

Clima 45+ /BP16C.

Clima 65+ /BP16D.

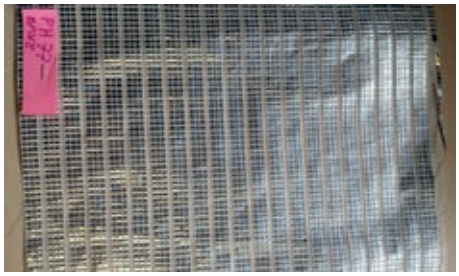

PH 77 /BP16E.

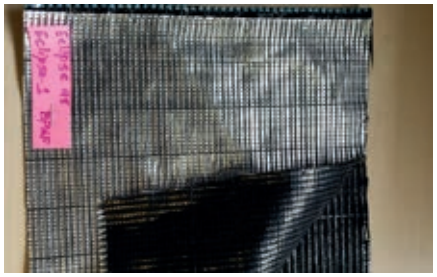

Eclipse 98 + Eclipse 1 /BP16F.

Figure 45 *Overview Low & Bonar screen samples.*

Saint Gobain-Cultilène
There are two samples provided by Saint Gobain-Cultilene. Both samples are made of glass fibre material but with different thickness:

- CU16O: AT40, the thin glass fibre screen.
- CU16P: this sample thicker than CU16O, was not coded by Cultilene.

An overview of Saint Gobain-Cultilene screens is presented in Figure 46.

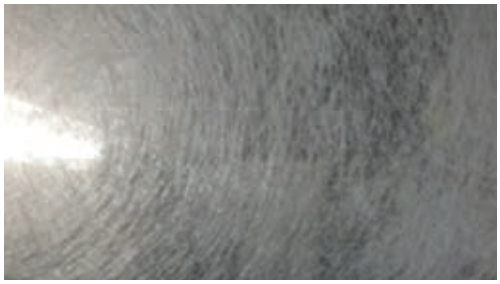

AT40, thin version of glassfibre sample / CU16O.

Thick version of glassfibre sample /CU16P.

Figure 46 *Overview Saint Gobain-Cultilene samples.*

Novavert
Novavert has provided 11 different sample:

- NT16C: Bühnenmolton mit Voll-Alu Beidseitig which is aluminized on both sides.
- NT16D: SHS Woven Clear mit Alustreifen is a completely closed screen made of aluminized and transparent woven bands.the repeating pattern is: 5xAl + 1x Tr.
- NT16E: HS 888 Modacryl mit 4 streifen is made of aluminized bands attached to a woven porous white screen. The repetition pattern is: 4xAl + 2xW.
- NT16F: HS 885 B3 Modacryl met 2 streifen is made of woven aluminized bands attached to a woven porous white screen. The repetition pattern is: 2xAl + 2xW.
- NT16G: SHS 115 B3 mit 2 Alustreifen is made of aluminized & transparent bands. The repeating pattern is as follows: 2xAl + 2xtr.
- NT16H: HS 885 ANTIFIRE B1 Trevira met 2 Streifen is made of matte (laminated) aluminized bands attached to a woven porous white screen. The repetition pattern is: 2xAl + 2xW.
- NT16I: WHS 115 is a woven screen made of equal parts of transparent and white bands.
- NT16J: WHS 115 +SHS 15 AntiFire B1 is made of two different screens attached to each other. Screen 1 is a woven transparent screen and screen 2 is screen WHs 115 (NT16I).
- NT16K: SHS 15 ANTIFIRE B1 is a woven transparent screen
- NT16L: SHS White Therm AntiFire B1 consists of 2 screens attached to each other. Screen 1 is a woven white screen and screen 2 is a woven diffuse screen.
- NT16M: Glasfasergewebe is a woven porous white screen.

The overview of Novavert samples is presented in Figure 47.

Bühnenmolton mit Voll-Alu Beidseitig /NT16C.

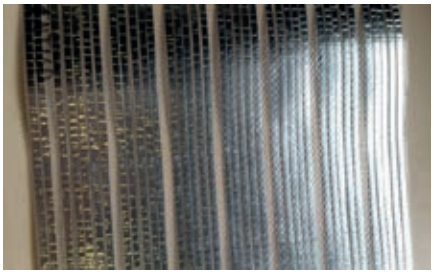

SHS Woven Clear mit Alustreifen /NT16D.

HS 888 Modacryl mit 4 streifen /NT16E.

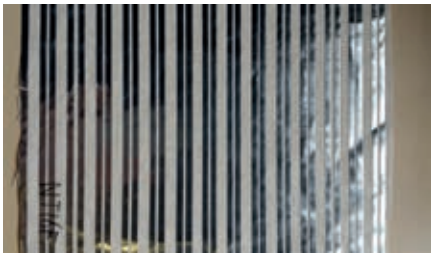

HS 885 B3 Modacryl met 2 streifen /NT16F.

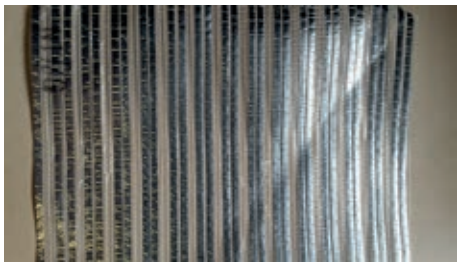

SHS 115 B3 mit 2 Alustreifen /NT16G.

HS 885 ANTIFIRE B1 Trevira met 2 Streifen / NT16H.

WHS 115 /NT16I.

WHS 115 +SHS 15 AntiFire B1 /NT16J.

SHS 15 ANTIFIRE B1 /NT16K.

SHS White Therm AntiFire B1 /NT16L.

Glasfasergewebe /NT16M.

***Figure 47** Overview Novavert samples.*

Ludvig Svensson

We have received 11 different samples from Ludvig Svensson. The WUR codes and descriptions of samples are listed below:

- LS16U : Luxous 1347 FR is a transparent woven screen.
- LS16V : Luxous 1347 H2NO FR is a transparent woven screen.
- LS16W : Harmony 2047 FR is a diffuse woven screen.
- LS16X : Harmony 4647 FR is made of equal parts of white and transparent bands.
- LS16Y : Harmony 7247 FR is a white screen.
- LS16Z : Tempa 5555 FR is made of equal parts of aluminized and transparent bands.
- LS16Z1: Tempa 8570 FR is made of aluminized and transparent bands. The repeatin pattern is: 7xAl + 1x Tr
- LS16Z2: Obscura 9950 FR W is made of white non-transparent bands woven with black and transparent threads. Both sides of screen are white.
- LS16Z3: Obscura 10070 FR WB + BW is a light blocking screen, white on one side and black on the other side.
- LS16Z4: Obscura 10075 FR AB + B consists of two screens. Screen 1 is a one sided aluminized screen with a black background and screen 2 is a woven black screen.

An overview of Ludvig Svensson samples is listed in Figure 48.

Luxous 1347 FR /LS16U.

Luxous 1347 H2NO FR /LS16V.

Harmony 2047 FR /LS16W.

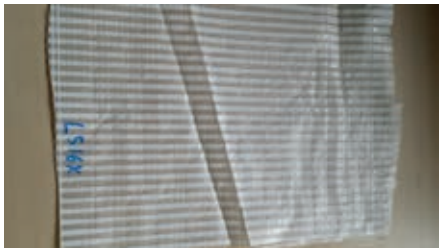

Harmony 4647 FR /LS16X.

Harmony 7247 FR /LS16Y.

Tempa 5555 FR /LS16Z.

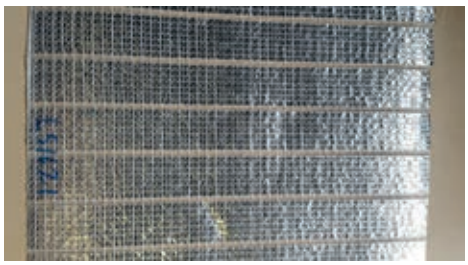

Tempa 8570 FR /LS16Z1.

Obscura 9950 FR W /LS16Z2.

Obscura 10070 FR WB + BW /LS16Z3.

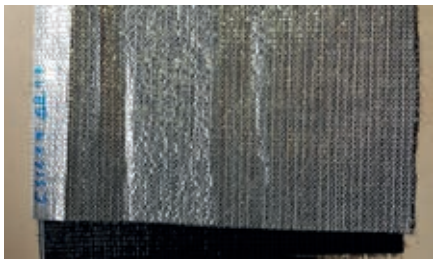

Obscura 10075 FR AB + B /LS16Z4.

Figure 48 *Overview Ludvig Svensson samples.*

Annex 2 Detailed description of model fitting procedure used to determine air permeability and resulting uncertainties

After the measurement of air permeability with the air suction device (2.3.4 and 2.3.5), the data is further processed in Excel. Even though the r^2-value in our example data in Figure 11D is 1.0000 a margin of error in the permeability and inertial factor has to be calculated since this r^2-value is only the proportion of explained variance and does not indicate the accuracy of the coefficients. We can obtain an accuracy by using the standard error (which is generated by excel using "Data" → "Data analysis" → "regression", an excerpt of the generated report is shown in the table below), this standard error is the standard deviation of the least squares estimate of the coefficient.

Table 30

Excerpt from regression report produced by excel data analysis toolbox showing not only the coefficients but also the standard deviation of the least squares estimate of these coefficients.

	Coefficients	*Standard Error*
Intercept	0	#N/A
X Variable 1	14.6232	0.0802
X Variable 2	56.8546	1.4726

In order to obtain a confidence level of 99% it is necessary to use 3 times this standard error to calculate the margin of error resulting from regression via:

$$marginmarginMargin\ of\ error = \frac{f(C1 \pm eC1) - f(C1)}{f(C1)} \cdot 100\%$$

$$Margin\ of\ error = \frac{f\big((C1 \pm eC1), (C2 \pm eC2)\big) - f(C1, C2)}{f(C1, C2)} \cdot 100\%$$

Where f(C1) and f(C1,C2) are the functions to calculate the permeability and Inertial factor. This results in 2 and 4 values for the margin of error for the permeability and inertial factor respectively, the largest of these sets are reported.

For our example data (showing an r^2-value of 1.0000) this polynomial regression results in a margin of error of 1.7% for the calculated permeability and 8.7% for the Inertial factor to be added to the margins of error stated by the sensor manufacturers. The resulting margin of error is larger for the calculated inertial factor simply because the domain that has been characterised is dominated by the Darcy relationship and there is almost no contribution from the quadratic term in the Darcy-Forchheimer relation in this domain. Because of this the low speed wind tunnel is deemed unfit to determine the inertial factor of screens.

As an illustration, the example measurement data and the polynomial trend line with its 99% confidence range is plotted in the Figure below.

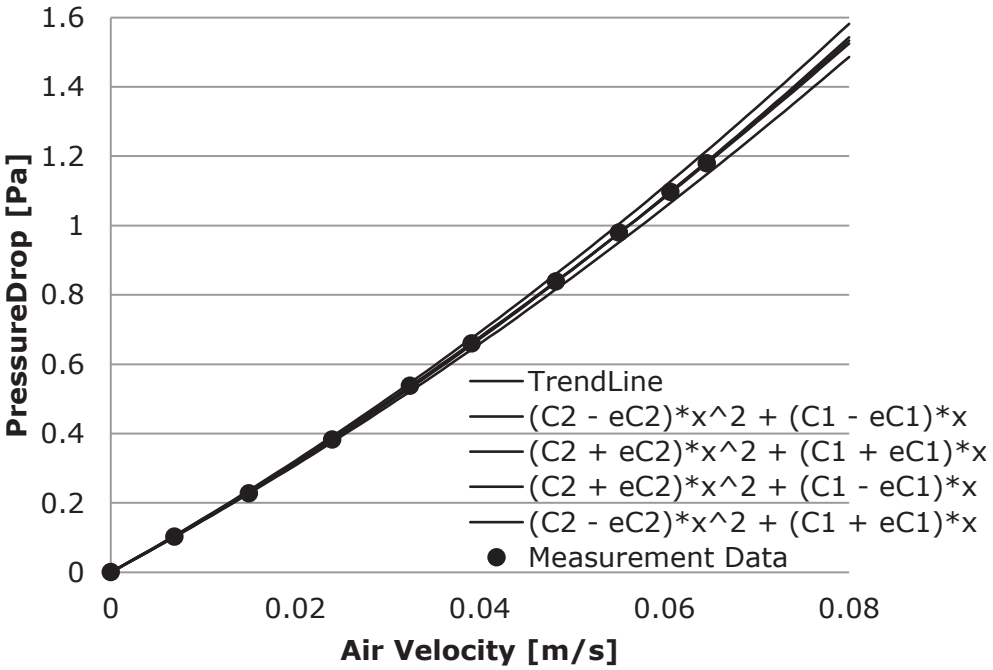

Figure 49 *Example of the measured pressure drop – air velocity relationship which can be described by the Forchheimer-Darcy model of flow through a porous media and has been fitted into the data as a trend line, also shown are the limits based on the standard error in the coefficients.*

In order to compare the results from the low speed and the high speed wind tunnel tests these standard errors and additional trend lines become very helpful and explain a lot of the differences in deduced permeability. The low speed and high speed wind tunnel measure the same characteristic pressure loss and wind speed relationship but over a different range of air speeds, afterwards the same Forchheimer-Darcy model is fitted into both data sets and the same 2 material characteristics are deduced (the permeability and the Inertial factor). In the Figure below this relationship as measured in the two wind tunnels is plotted in the same graph.

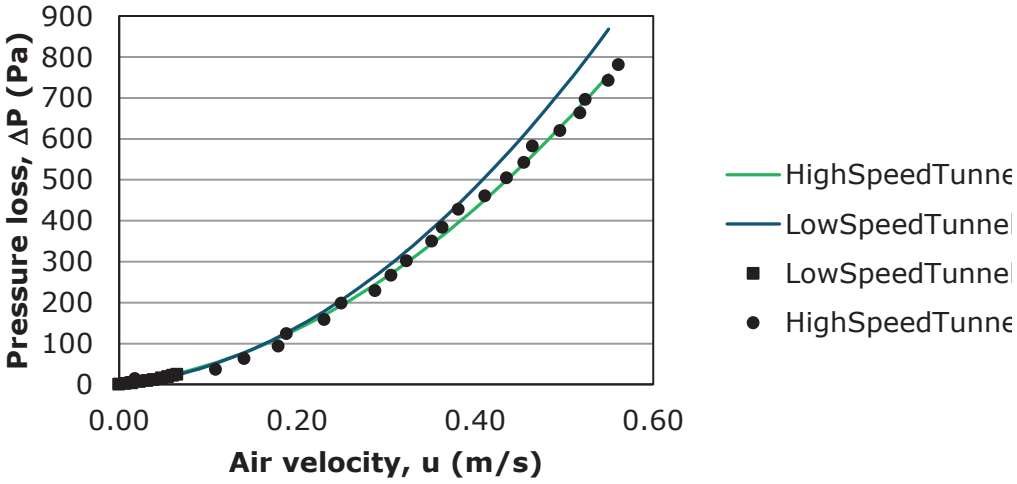

Figure 50 *Pressure loss and air velocity relationship of sample LS16U as characterised by both the low speed and high speed wind tunnel experiments and their fitted trend lines. The trend lines based on the high speed and low speed wind tunnels have respective r2-values of 0.9973 and 1.0000, indicating an extremely high proportion of explained variance.*

On initial evaluation, the data from both wind tunnels seem to be in good agreement, the trend line from the high speed wind tunnel passes straight through the results from the low speed wind tunnel and even the trend line from the low speed wind tunnel stays near the data points from the high speed wind tunnel despite the fact that it is being extrapolated ten times the range on which the trend line has been established. One could barely wish for a better agreement, but unfortunately the deduced permeability's do show very different values.

Table 31

Permeability values deduced from high and low speed wind tunnel experiments for sample LS16U.

	Deduced permeability	r^2-value of fitted trend lines
Low speed wind tunnel	$6.69 \cdot 10^{-8}\,m^2$	1.0000
High speed wind tunnel	$9.14 \cdot 10^{-8}\,m^2$	0.9973

If we apply the method described earlier in this section and take the standard deviation of the least squares estimate of the coefficients into account instead of the proportion of explained variance (r^2) it will become clear that there is actually a rather large margin of uncertainty that results from the regression analysis.

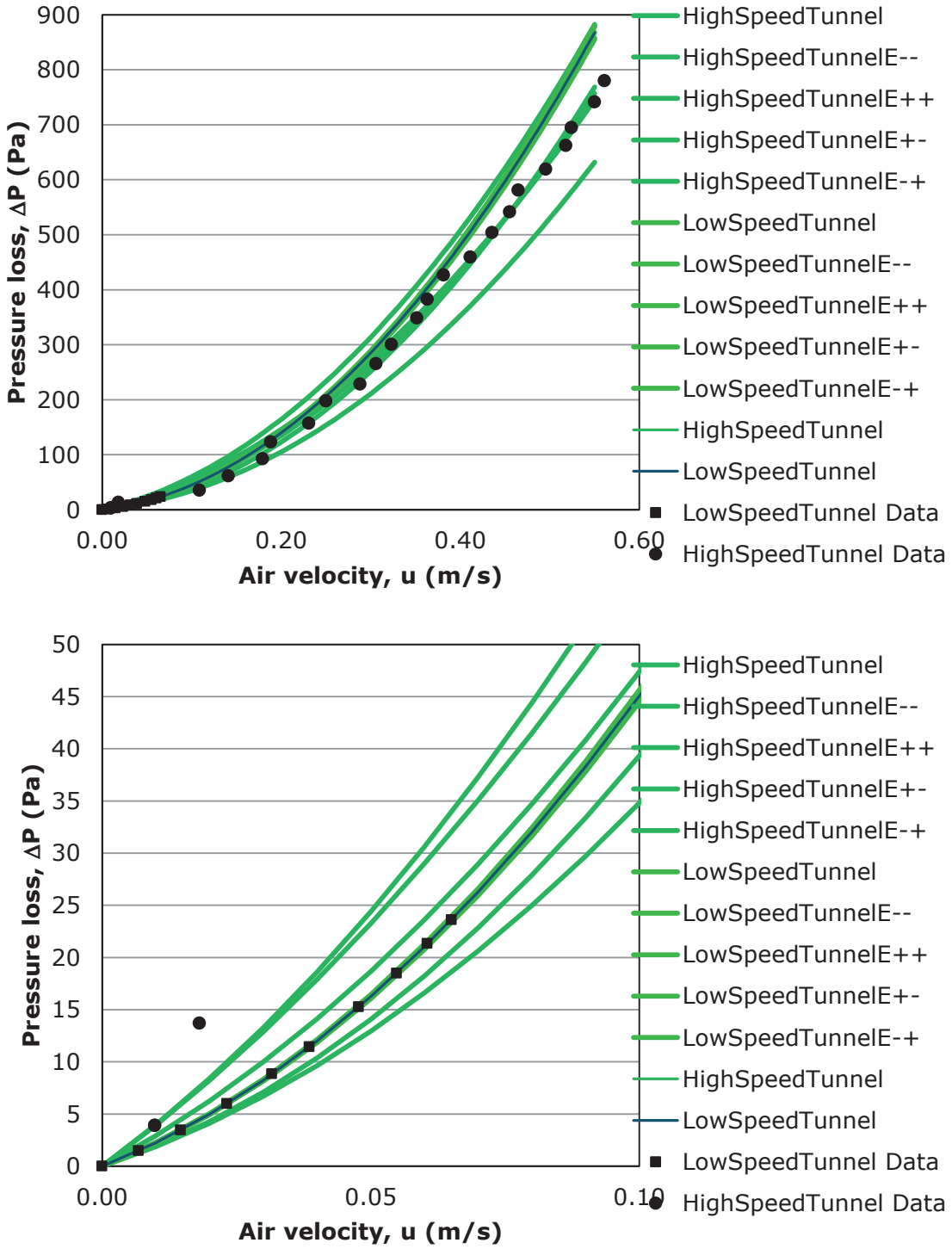

Figure 51 *Pressure loss and air velocity relationship of sample LS16U as characterised by both the low speed and high speed wind tunnel experiments as shown earlier but with added trend lines showing the actual uncertainty as a result from the regression analysis. Above the entire range is plotted encompassing the range of both wind tunnels, below the same figure is shown zoomed in on the range of the low speed wind tunnel.*

In the Figure above it is clearly visible that the possible trend lines from the high speed wind tunnel encompasses the results from the low speed wind tunnel. If we express this margin of uncertainty as a percentage it is also clear that the data overlaps.

Table 32

Permeability values deduced from high and low speed wind tunnel experiments for sample LS16U together with the uncertainty introduced by the regression analysis.

	Deduced permeability	Uncertainty range based on 3 times the standard deviation of the least squares estimate of the coefficients
Low speed wind tunnel	$6.69 \cdot 10^{-8}\,m^2$	1 %
High speed wind tunnel	$9.14 \cdot 10^{-8}\,m^2$	61 %

To explore the potential of nature to improve the quality of life

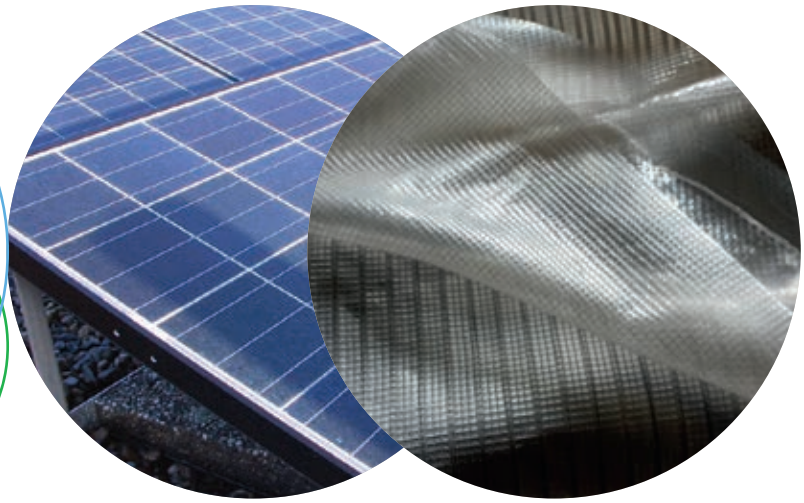

Wageningen University & Research,
BU Greenhouse Horticulture
P.O. Box 20
2665 ZG Bleiswijk
Violierenweg 1
2665 MV Bleiswijk
The Netherlands
T +31 (0)317 48 56 06
F +31 (0)10 522 51 93
www.wageningenur.nl/glastuinbouw

Greenhouse Horticulture Report GTB-1431

Wageningen University & Research, BU Greenhouse Horticulture initiates and stimulates innovations for a sustainable protected horticulture and a better quality of life. This is achieved by partnering with primary producers, the supply sector, plant breeding companies, the scientific community and governments in applied research.

The mission of Wageningen University & Research is 'To explore the potential of nature to improve the quality of life'. Within WUR, nine specialised research institutes of the DLO Foundation have joined forces with WUR to help answer the most important questions in the domain of healthy food and living environment. With approximately 30 locations, 6,000 members of staff and 9,000 students, WUR is one of the leading organisations in its domain worldwide. The integral approach to problems and the cooperation between the various disciplines are at the heart of the unique Wageningen Approach.